

Multivariate time-series modeling with generative neural networks

Marius Hofert¹, Avinash Prasad², Mu Zhu³

2021-10-05

Abstract

Generative moment matching networks (GMMNs) are introduced as dependence models for the joint innovation distribution of multivariate time series (MTS). Following the popular copula–GARCH approach for modeling dependent MTS data, a framework based on a GMMN–GARCH approach is presented. First, ARMA–GARCH models are utilized to capture the serial dependence within each univariate marginal time series. Second, if the number of marginal time series is large, principal component analysis (PCA) is used as a dimension-reduction step. Last, the remaining cross-sectional dependence is modeled via a GMMN, the main contribution of this work. GMMNs are highly flexible and easy to simulate from, which is a major advantage over the copula–GARCH approach. Applications involving yield curve modeling and the analysis of foreign exchange-rate returns demonstrate the utility of the GMMN–GARCH approach, especially in terms of producing better empirical predictive distributions and making better probabilistic forecasts.

Keywords

Generative moment matching networks, learning distributions, copulas, probabilistic forecasts, ARMA–GARCH model, yield curves, exchange-rate dependence.

MSC2010

62H99, 65C60, 60E05, 00A72, 65C10, 62M10.

1 Introduction

We extend the popular *copula–GARCH approach* (Jondeau and Rockinger 2006; Patton 2006) for modeling multivariate time series (MTS) data by replacing parametric copulas with generative neural networks. Our primary goal is to make probabilistic forecasts by constructing empirical predictive distributions. Quantities we are interested in forecasting include not just the average value but also quantiles, tail probabilities and others at any given time point in the future.

Copula–GARCH approach

Typically, there are two types of dependence in MTS data: serial dependence within each univariate time series, and cross-sectional dependence between the individual time series. A key feature of the copula–GARCH approach is that it models these two types of dependence separately.

¹Department of Statistics and Actuarial Science, University of Waterloo, 200 University Avenue West, Waterloo, ON, N2L 3G1, marius.hofert@uwaterloo.ca. The author acknowledges support from NSERC (Grant RGPIN-2020-04897).

²Department of Statistics and Actuarial Science, University of Waterloo, 200 University Avenue West, Waterloo, ON, N2L 3G1, a2prasad@uwaterloo.ca. The author acknowledges support from NSERC (PGS D Scholarship).

³Department of Statistics and Actuarial Science, University of Waterloo, 200 University Avenue West, Waterloo, ON, N2L 3G1, mu.zhu@uwaterloo.ca. The author acknowledges support from NSERC (RGPIN-2016-03876).

First, for serial dependence within each univariate time series, the copula–GARCH approach uses a class of generalized auto-regressive conditional heteroscedasticity (GARCH) models (Bollerslev 1986). While there is a plethora of literature on univariate time series modeling with a wide range of models that are tailor-made for capturing various types of serial patterns such as seasonality, volatility clustering or regime switching, GARCH-type models are popular choices in the realm of financial econometrics because they are designed to account for various stylized facts (such as volatility clustering) that are often present in financial return series data; see McNeil et al. (2015, Chapter 3).

Second, for cross-sectional dependence between the individual time series, the copula–GARCH approach leverages Sklar’s Theorem (Sklar 1959) to allow the use of any copula to model the joint innovation distribution. This extends various classic approaches (e.g., Bollerslev 1990; Engle 2002; Tse and Tsui 2002) that rely on the multivariate normal distribution to model the cross-sectional dependence, and is the main attraction that makes the copula–GARCH approach a highly flexible modeling approach. For a brief overview of its versatility and popularity in the context of finance and econometrics, see Patton (2012); for the calibration of these models, see Aas (2016), Almeida et al. (2016), as well as Oh and Patton (2017).

Motivation

While there is a growing collection of copula models to characterize complex dependence structures, most of them are already limited in moderately large dimensions and often do not provide an adequate fit to given data (e.g., Hofert and Oldford 2018). Identifying appropriate copula models, estimating their parameters and, especially, testing their goodness-of-fit and selecting the final model are time-consuming at best. These modeling steps often require sophisticated algorithms but still do not lead to an adequate model among the computationally tractable ones. To address these shortcomings, we propose to replace parametric copula models in the copula–GARCH approach with a generative moment matching network (GMMN). In comparison to parametric copulas, GMMNs can capture a much larger variety of complex dependence structures. We call this alternative modeling approach the *GMMN–GARCH approach*.

For high-dimensional MTS data, we also incorporate principal component analysis (PCA) as an intermediate step to reduce the dimensionality; although other dimension reduction techniques, such as autoencoders, can be used here as well, we do not focus on this aspect in the current paper. Thus, our proposed GMMN–GARCH approach consists of the following three components:

- 1) serial dependence modeling — while many possibilities can be considered, here we deliberately do not deviate from the copula–GARCH approach and use marginal ARMA–GARCH models;
- 2) dimension reduction (optional) — several choices are available, but when this step is needed we simply apply PCA; and
- 3) cross-sectional dependence modeling — here, the copula–GARCH approach would choose a parametric copula, but we introduce the use of GMMNs, the main contribution of this paper.

Related use of neural networks

Neural networks have appeared in the time series literature before. For example, quite a few research groups have used neural networks to replace the aforementioned GARCH model for serial dependence marginally within each individual time series (e.g., Lua et al. 2016; Liu and So 2020). Another common use of neural networks for time series data is to model not only the serial dependence marginally within each individual time series, but also their conditional relationships with multiple covariates,

which themselves may be time series, too (e.g., Chaudhuri and Ghosh 2016; Yu and Chang 2020). By contrast, we use neural networks to replace the copula model for cross-sectional dependence jointly between individual time series, and make improved probabilistic forecasts as a result. We are not yet aware of such attempts in the literature.

Neural networks also have been used by, for example, Ling et al. (2020) in the context of copula modeling. Our work differs from theirs in two ways. First, they learn their copulas in a static setting, not in the context of MTS data. Second, they restrict themselves to Archimedean copulas (which are copulas representable as $C(u_1, \dots, u_d) = \psi(\psi^{-1}(u_1) + \dots + \psi^{-1}(u_d))$ with certain conditions on ψ), and only use neural networks to learn the underlying generator (the function ψ). While a nonparametric generator can give considerable flexibility to the corresponding Archimedean copula, it is not fully flexible as clearly not all dependence structures are Archimedean.

Organization

In Section 2, we outline our framework for modeling MTS data. In particular, we focus on the novel integration of GMMNs within this framework. In Section 3, we discuss how to make probabilistic forecasts and evaluate the performance of our MTS model. Then in Section 4, we showcase our GMMN-based multivariate time series model in applications to yield curve and exchange-rate data. Section 5 provides concluding remarks.

2 Framework for multivariate time series modeling

Let $(\mathbf{X}_t)_{t \in \mathbb{Z}}$ denote a d -dimensional time series of interest, where $\mathbf{X}_t = (X_{t,1}, \dots, X_{t,d})$. Furthermore, consider a stretch of τ realizations from $(\mathbf{X}_t)_{t \in \mathbb{Z}}$ denoted by $\mathbf{X}_1, \dots, \mathbf{X}_\tau$. For applications in finance, these are often log-returns of d asset prices (and negative log-returns for applications in risk management); see Section 4 for more details. In this section, we describe in more depth the three modeling components outlined in Section 1 above.

2.1 Modeling serial dependence

The *ARMA–GARCH models* in Step 1) are ARMA models with GARCH errors; see McNeil et al. (2015, Section 4.2.3). An $\text{ARMA}(p_{1j}, q_{1j})\text{--GARCH}(p_{2j}, q_{2j})$ model has the form

$$\begin{aligned} X_{t,j} &= \mu_{t,j} + \sigma_{t,j} Z_{t,j}, \\ \mu_{t,j} &= \mu_j + \sum_{k=1}^{p_{1j}} \phi_{jk}(X_{t-k,j} - \mu_j) + \sum_{l=1}^{q_{1j}} \gamma_{jl}(X_{t-l,j} - \mu_{t-l,j}), \\ \sigma_{t,j}^2 &= \omega_j + \sum_{k=1}^{p_{2j}} \alpha_{jk}(X_{t-k,j} - \mu_{t-k,j})^2 + \sum_{l=1}^{q_{2j}} \beta_{jl} \sigma_{t-l,j}^2, \end{aligned}$$

where, for each component $j = 1, \dots, d$, one has $\mu_j \in \mathbb{R}$, $\omega_j > 0$, and $\alpha_{jk}, \beta_{jl} \geq 0$ for all k, l . Additional conditions on the coefficients ϕ_{jk} , γ_{jl} , α_{jk} and β_{jl} are necessary to ensure that the ARMA–GARCH processes are causal and covariance stationary; see, e.g., McNeil et al. (2015, Section 4.1.2–4.2.2) for the details. For each $j = 1, \dots, d$, the *innovations* $Z_{t,j}$ in the definition of the ARMA–GARCH model are independent and identically distributed (iid) random variables with $\mathbb{E}(Z_{t,j}) = 0$ and $\text{Var}(Z_{t,j}) = 1$; their realizations after fitting marginal $\text{ARMA}(p_{1j}, q_{1j})\text{--GARCH}(p_{2j}, q_{2j})$ models are known as *standardized residuals* and denoted by $\hat{Z}_{t,j}$, $t = 1, \dots, \tau$ and $j = 1, \dots, d$. In financial time series applications,

common choices of innovation distributions include the standard normal, the scaled t and the skewed t distribution.

Fitting marginal time series models is typically done by fitting low-order models with likelihood-based methods and selecting the most adequate fit using the AIC/BIC model selection criterion among the candidate models. A popular broad-brush approach is to fit a GARCH(1, 1) model for financial return series — specifically, an ARMA(0, 0)–GARCH(1, 1) model in our context — and continue the modeling based on the standardized residuals $\hat{Z}_{1,j}, \dots, \hat{Z}_{\tau,j}$; see McNeil et al. (2015, Chapter 4) or Hofert, Kojadinovic, et al. (2018, Section 6.2.3). This procedure is also referred to as *deGARCHing*. With the help of model diagnostic tools — for example, plots of the autocorrelation function (ACF) of $\hat{Z}_{1,j}, \dots, \hat{Z}_{\tau,j}$ and that of their squared values, Ljung–Box tests or an assessment of the innovation distribution through Q-Q plots — one can then assess the adequacy of each marginal time series model. In what follows we use $\hat{\mu}_{t,j}$ and $\hat{\sigma}_{t,j}^2$ to denote the estimated conditional mean and variance models for the j th marginal time series with orders $\hat{p}_{1j}, \hat{q}_{1j}, \hat{p}_{2j}, \hat{q}_{2j}$ and fitted parameters $\hat{\phi}_{jk}, \hat{\gamma}_{jl}, \hat{\alpha}_{jk}, \hat{\beta}_{jl}$.

Having accounted for the marginal serial dependence in this way, the subsequent analysis in our modeling framework will operate on the standardized residuals $\hat{\mathbf{Z}}_t = (\hat{Z}_{t,1}, \dots, \hat{Z}_{t,d})$, $t = 1, \dots, \tau$, which are themselves realizations of the innovation random variables, $\mathbf{Z}_1, \dots, \mathbf{Z}_\tau$, assumed to be iid in the copula–GARCH approach.

Note that any other adequate marginal time series modeling approach can be applied in our framework as long as the model’s marginal residuals can be considered to be iid realizations from a continuous distribution. Our choice of ARMA–GARCH models here and in what follows is motivated only from the fact that these are the most popular marginal time series models used in practice.

2.2 Dimension reduction

Two popular dimension-reduction techniques for multivariate financial time series are factor models and PCA; see McNeil et al. (2015, Chapter 6) and the references therein for a brief summary. An approach that is perhaps less discussed in the financial econometrics literature involves using autoencoder neural networks for dimension reduction in which two separate neural network mappings are learned to and from the lower dimensional space; see Hinton and Salakhutdinov (2006). As dimension reduction is not our main contribution in this work, we simply utilize PCA in what follows.

Note that PCA is often applied to the MTS data $\mathbf{X}_1, \dots, \mathbf{X}_\tau$ in the literature; see, e.g., Alexander (2000). Apart from reducing the burden of marginal time series modeling, there is no strong reason why PCA should be applied to potentially non-stationary data. If dimension reduction is necessary, we find it statistically more sound to apply PCA to the standardized residuals $\hat{\mathbf{Z}}_t$ after first accounting for any serial dependence in the marginal time series.

Let $\hat{\Sigma}$ denote the sample covariance matrix of the standardized residuals $\hat{\mathbf{Z}}_t$, $t = 1, \dots, \tau$. The result from PCA is the matrix $\hat{\Gamma} \in \mathbb{R}^{d \times d}$ whose columns consist of the eigenvectors of $\hat{\Sigma}$, sorted according to decreasing eigenvalues $\hat{\lambda}_1 \geq \dots \geq \hat{\lambda}_d \geq 0$. For the purposes of dimension reduction, $\hat{\mathbf{Z}}_t$, $t = 1, \dots, \tau$, are transformed to $\hat{\mathbf{Y}}_t = \hat{\Gamma}_{:,1:k}^\top \hat{\mathbf{Z}}_t$, where $\hat{\Gamma}_{:,1:k} \in \mathbb{R}^{d \times k}$ represent the first k columns of $\hat{\Gamma}$ for some $1 \leq k < d$. As a result, the sample covariance matrix of \mathbf{Y}_t is (approximately) diagonal, and the components of \mathbf{Y}_t are (approximately) uncorrelated. The j th component series $Y_{1,j}, \dots, Y_{\tau,j}$, forms realizations of the j th principal component, and the first k principal component series account for $\sum_{j=1}^k \hat{\lambda}_j / \sum_{j=1}^d \hat{\lambda}_j$ of the total variance.

As dimension reduction is an optional component in our modeling framework, the next step involves dependence modeling of either the standardized residuals $\hat{\mathbf{Z}}_1, \dots, \hat{\mathbf{Z}}_\tau$ directly or their principal components $\hat{\mathbf{Y}}_1, \dots, \hat{\mathbf{Y}}_\tau$. To unify the notation for both cases, we define a d^* -dimensional time series $\hat{\mathbf{Y}}_t = \hat{\Gamma}^\top \hat{\mathbf{Z}}_t$, where $\hat{\Gamma} = \hat{\Gamma}_{:,1:k}$ if dimension reduction is employed and $\hat{\Gamma} = I_d$ (the identity matrix

in $\mathbb{R}^{d \times d}$) otherwise; consequently, $d^* = k$ in the former case and $d^* = d$ in the latter. Furthermore, we treat $\hat{\mathbf{Y}}_1, \dots, \hat{\mathbf{Y}}_\tau$ as realizations from \mathbf{Y}_t and so naturally, $\mathbf{Y}_t = \Upsilon^\top \mathbf{Z}_t$ with $\Upsilon = \Gamma_{\cdot, 1:k}$ if dimension reduction is used and $\Upsilon = I_d$ otherwise.

2.3 Modeling cross-sectional dependence

The final task in our framework involves the modeling of the iid series $\mathbf{Y}_1, \dots, \mathbf{Y}_\tau$. To account for cross-sectional dependence, we model the joint distribution function H of \mathbf{Y}_t using Sklar's Theorem as

$$H(\mathbf{y}) = C(F_1(y_1), \dots, F_{d^*}(y_{d^*})), \quad \mathbf{y} \in \mathbb{R}^{d^*},$$

where F_j , $j = 1, \dots, d^*$, are the margins of H and $C : [0, 1]^{d^*} \rightarrow [0, 1]$ is the copula of $(Y_{t,1}, \dots, Y_{t,d^*})$ for each t .

Following a classical copula modeling approach, one first builds the *pseudo-observations* $\hat{U}_{t,j} = R_{t,j}/(\tau + 1)$, $t = 1, \dots, \tau$, $j = 1, \dots, d^*$, where $R_{t,j}$ denotes the rank of $\hat{Y}_{t,j}$ among $\hat{Y}_{1,j}, \dots, \hat{Y}_{\tau,j}$. The pseudo-observations are viewed as realizations from C based on which one would fit candidate copula models; see, e.g., McNeil et al. (2015, Section 7.5.1) or Hofert, Kojadinovic, et al. (2018, Section 4.1.2). Note that by considering the non-parametric pseudo-observations (even in the case when we do not apply a dimension reduction technique and thus know the (fitted) marginal innovation distributions), we reduce the risk of a misspecified margin affecting the estimation of the copula C ; see Genest and Segers (2010) for a theoretical justification of this approach. Therefore, going forward, we will use the pseudo-observations $\hat{\mathbf{U}}_t = (\hat{U}_{t,1}, \dots, \hat{U}_{t,d^*})$, $t = 1, \dots, \tau$, to model the cross-sectional dependence structure of $\hat{\mathbf{Y}}_t$.

2.3.1 Parametric copulas

A traditional approach for modeling the cross-sectional dependence described by $\hat{\mathbf{U}}_1, \dots, \hat{\mathbf{U}}_\tau$ involves the fitting of parametric copula models, their goodness-of-fit assessment and finally, model selection. There are numerous families of copula models to consider depending on prominent features of the dependence structure present in $\hat{\mathbf{U}}_t$ such as (a)symmetries or a concentration of points in the lower/upper tail of the joint distribution (or pairs of such) which hints at an adequate model possessing tail dependence.

A problem with this approach is that it is often hard to find an adequate copula model for given real-life data, especially in higher dimensions where typically some pairwise dependencies contradict the corresponding model-implied marginal copulas; see, e.g., Hofert and Oldford (2018). Another problem is that certain copula models are computationally expensive to fit and test for goodness-of-fit. In Section 4, we investigate whether (the much more flexible) GMMNs can outperform prominent elliptical and Archimedean copulas, as well as flexible vine copulas constructed using trees of bivariate copulas (Dissmann et al. 2013; Aas et al. 2009), in the context of our framework. In what follows we thus shall denote by \hat{C}_{PM} a (generic) parametric copula model fitted to the pseudo-observations $\hat{\mathbf{U}}_1, \dots, \hat{\mathbf{U}}_\tau$.

2.3.2 Nonparametric copulas

Nonparametric copulas, which are more flexible in nature than their parametric counterparts, can also be used to model cross-sectional dependence. A simple and standard nonparametric estimator of C is the empirical copula, which is merely the empirical distribution function of the pseudo-observations $\hat{\mathbf{U}}_1, \dots, \hat{\mathbf{U}}_\tau$. Since the empirical copula can exhibit large bias when the sample size is small, we also consider a smoothed version of it, known as the empirical beta copula (Segers et al. 2017), which is a

member of the class of empirical Bernstein copulas (Sancetta and Satchell 2004). The smoothness of the empirical beta copula is a consequence of replacing the indicator functions in the empirical distribution function with a product of various beta distribution functions. Going forward, we use \hat{C}_{NPM} to denote a (generic) nonparametric estimator of the target copula C .

2.3.3 GMMNs

We propose to utilize generative neural networks (in particular, GMMNs) for modeling the cross-sectional dependence structure of the pseudo-observations $\hat{U}_1, \dots, \hat{U}_\tau$. In our framework, a generative neural network $f_{\hat{\theta}}$ with fitted parameter vector $\hat{\theta}$ is used as an estimator for the distribution of the pseudo-observations. Let \hat{C}_{NN} denote the empirical copula based on a sample generated from a trained GMMN $f_{\hat{\theta}}$.

GMMNs, also known as Maximum Mean Discrepancy (MMD) nets, were introduced simultaneously by Li et al. (2015) and Dziugaite et al. (2015). A GMMN f_{θ} utilizes a kernel maximum mean discrepancy statistic as the *loss function* to learn the distribution of the pseudo-observations. Conceptually, f_{θ} can be thought of as a parametric map from a random vector $\mathbf{V}_t = (V_{t,1}, \dots, V_{t,p})$ with (known) *prior distribution* $F_{\mathbf{V}}$ to $\hat{\mathbf{U}}_t = (\hat{U}_{t,1}, \dots, \hat{U}_{t,d^*})$. As is standard in the literature, we assume that $V_{t,1}, \dots, V_{t,p}$ are iid. Typical choices of $F_{\mathbf{V}}$ are $U(0, 1)$ or $N(0, 1)$; we utilize the latter. Based on the fitted GMMN $f_{\hat{\theta}} : \mathbb{R}^p \rightarrow [0, 1]^{d^*}$ we can then generate samples with copula \hat{C}_{NN} as an approximation to the target copula C of $\hat{\mathbf{U}}_t$. As demonstrated in Hofert, Prasad, et al. (2021), GMMNs provide a flexible class of models capable of learning a variety of complex dependence structures.

In this paper, we work with a *feedforward neural network* (also known as the multi-layer perceptron), which we simply refer to as *neural network (NN)* in what follows. For details pertaining to the mathematical representation of these NNs, see Appendix A. Having established the architecture of f_{θ} , we will now briefly discuss the loss function and training procedure used for estimating θ .

Loss function

To learn f_{θ} , we work with τ training data points consisting of the pseudo-observations $\hat{\mathbf{U}}_1, \dots, \hat{\mathbf{U}}_\tau$. Given an input sample $\mathbf{V}_1, \dots, \mathbf{V}_{n_{\text{gen}}}$ from the prior distribution $F_{\mathbf{V}}$, the GMMN generates an output sample $\mathbf{U}_1, \dots, \mathbf{U}_{n_{\text{gen}}}$, where $\mathbf{U}_t = f_{\theta}(\mathbf{V}_t)$, $t = 1, \dots, n_{\text{gen}}$. In selecting an appropriate loss function, we are naturally interested in measuring whether the two samples $\hat{\mathbf{U}} = (\hat{\mathbf{U}}_1^\top, \dots, \hat{\mathbf{U}}_\tau^\top)^\top \in [0, 1]^{\tau \times d^*}$ and $\mathbf{U} = (\mathbf{U}_1^\top, \dots, \mathbf{U}_{n_{\text{gen}}}^\top)^\top \in [0, 1]^{n_{\text{gen}} \times d^*}$ can be deemed to come from the same distribution.

To do so, GMMNs use the *maximum mean discrepancy (MMD)* as loss function, which was introduced as a two-sample test statistic by Gretton et al. (2007). For a given embedding function $\varphi : \mathbb{R}^{d^*} \mapsto \mathbb{R}^{d'}$, the MMD measures the distance between two sample statistics, $(1/\tau) \sum_{t_1=1}^{\tau} \varphi(\hat{\mathbf{U}}_{t_1})$ and $(1/n_{\text{gen}}) \sum_{t_2=1}^{n_{\text{gen}}} \varphi(\mathbf{U}_{t_2})$, in the embedded space $\mathbb{R}^{d'}$ via

$$\begin{aligned} & \text{MMD}(\hat{\mathbf{U}}, \mathbf{U}) \\ &= \left\| \frac{1}{\tau} \sum_{t_1=1}^{\tau} \varphi(\hat{\mathbf{U}}_{t_1}) - \frac{1}{n_{\text{gen}}} \sum_{t_2=1}^{n_{\text{gen}}} \varphi(\mathbf{U}_{t_2}) \right\|_2 \\ &= \left(\frac{1}{\tau^2} \sum_{t_1=1}^{\tau} \sum_{t_2=1}^{\tau} \varphi(\hat{\mathbf{U}}_{t_1})^\top \varphi(\hat{\mathbf{U}}_{t_2}) - \frac{2}{\tau n_{\text{gen}}} \sum_{t_1=1}^{\tau} \sum_{t_2=1}^{n_{\text{gen}}} \varphi(\hat{\mathbf{U}}_{t_1})^\top \varphi(\mathbf{U}_{t_2}) + \frac{1}{n_{\text{gen}}^2} \sum_{t_1=1}^{n_{\text{gen}}} \sum_{t_2=1}^{n_{\text{gen}}} \varphi(\mathbf{U}_{t_1})^\top \varphi(\mathbf{U}_{t_2}) \right)^{1/2}. \end{aligned}$$

If we can choose $\varphi(\cdot)$ to be a kind of “distributional embedding”, for example, in the sense that the two statistics — $(1/\tau) \sum_{t_1=1}^{\tau} \varphi(\hat{\mathbf{U}}_{t_1})$ and $(1/n_{\text{gen}}) \sum_{t_2=1}^{n_{\text{gen}}} \varphi(\mathbf{U}_{t_2})$ — contain all empirical moments of $\hat{\mathbf{U}}$

and U , respectively, then the MMD criterion can be used as a proxy for measuring whether the two samples have the same distribution.

By Mercer (1909), the inner product $\varphi(\hat{\mathbf{u}}_t)^\top \varphi(\mathbf{u}_t)$ can be computed in a reproducing kernel Hilbert space by $K(\hat{\mathbf{u}}_t, \mathbf{u}_t)$, where $K(\cdot, \cdot) : \mathbb{R}^{d^*} \times \mathbb{R}^{d^*} \mapsto \mathbb{R}$ denotes a kernel similarity function. Hence, for a given kernel function $K(\cdot, \cdot)$, the MMD statistic above is equivalent to

$$\text{MMD}(\hat{U}, U; K) = \left(\frac{1}{\tau^2} \sum_{t_1=1}^{\tau} \sum_{t_2=1}^{\tau} K(\hat{U}_{t_1}, \hat{U}_{t_2}) - \frac{2}{\tau n_{\text{gen}}} \sum_{t_1=1}^{\tau} \sum_{t_2=1}^{n_{\text{gen}}} K(\hat{U}_{t_1}, U_{t_2}) + \frac{1}{n_{\text{gen}}^2} \sum_{t_1=1}^{n_{\text{gen}}} \sum_{t_2=1}^{n_{\text{gen}}} K(U_{t_1}, U_{t_2}) \right)^{1/2}. \quad (1)$$

If $K(\cdot, \cdot)$ is chosen to be a so-called universal kernel function, such as a Gaussian or Laplace kernel, then the associated implicit embedding $\varphi : \mathbb{R}^{d^*} \mapsto \mathbb{R}^\infty$ is indeed a “distributional embedding” in the sense described above, and one can show that the MMD converges in probability to 0 for $\tau, n_{\text{gen}} \rightarrow \infty$ if and only if $\hat{C}_{\text{NN}} = C$ (Gretton et al. 2007; Gretton et al. 2012).

As suggested by Li et al. (2015), we opt to work with a mixture of Gaussian kernels (rather than a single Gaussian kernel) with different bandwidth parameters,

$$K(\hat{\mathbf{u}}_t, \mathbf{u}_t) = \sum_{i=1}^{n_{\text{krr}}} K(\hat{\mathbf{u}}_t, \mathbf{u}_t; \sigma_i), \quad (2)$$

where n_{krr} denotes the number of mixture components and $K(\hat{\mathbf{u}}_t, \mathbf{u}_t; \sigma) = \exp(-\|\hat{\mathbf{u}}_t - \mathbf{u}_t\|_2^2 / (2\sigma^2))$ is the Gaussian kernel with bandwidth parameter $\sigma > 0$.

Thus, to train the GMMN $f_{\boldsymbol{\theta}}$, we perform the optimization

$$\min_{\boldsymbol{\theta}} \text{MMD}(\hat{U}, (f_{\boldsymbol{\theta}}(V); K_{\text{trn}}), \quad (3)$$

where $V = (\mathbf{V}_1^\top, \dots, \mathbf{V}_{n_{\text{gen}}}^\top)^\top \in [0, 1]^{n_{\text{gen}} \times p}$, the NN transform $f_{\boldsymbol{\theta}}$ is understood to be applied row-wise, and K_{trn} represents the selected mixture of Gaussian kernels used to train the GMMN. The specific choice of the number of mixture components n_{krr} and the bandwidth parameters σ_i , $i = 1, \dots, n_{\text{krr}}$ that characterize K_{trn} will be provided in Section 4.

Training GMMNs

We now discuss how we can train the GMMN $f_{\boldsymbol{\theta}}$, that is, how we can estimate the parameter vector $\boldsymbol{\theta}$. For the sake of convenience, we always simply set $n_{\text{gen}} = \tau$ while training the GMMN. (However, after training we can still generate an arbitrary number of samples from $f_{\hat{\boldsymbol{\theta}}}$.)

Directly optimizing the MMD loss function in (1), also known as batch optimization, would involve all $\binom{\tau}{2}$ pairs of observations which is memory-prohibitive even for moderately large τ . While the Nyström approximation is commonly used to reduce the storage and computational cost of large kernel matrices, it is not a desirable approach for us. This is because, for conventional kernel methods such as support vector machines, the kernel matrix itself is often fixed — and hence precomputed — for the corresponding optimization problem, but this is not the case for our optimization problem (3). Instead, we adopt a mini-batch optimization procedure, where we partition the training dataset into *batches* of size n_{bat} and use the batches sequentially to update $\boldsymbol{\theta}$. After all the training data are exhausted, that is, roughly (τ/n_{bat}) -many gradient steps, one epoch of the training of the GMMN is completed. Batch optimization results as a special case of this mini-batch optimization procedure when we set $n_{\text{bat}} = \tau$; it can be used with relatively small datasets. To update the parameter vector $\boldsymbol{\theta}$, we utilize

the Adam optimizer of Kingma and Ba (2014) which uses a “memory-sticking gradient” procedure — a weighted combination of the current gradient and past gradients from earlier iterations. The trade-off in utilizing mini-batches, particularly with a smaller batch size n_{bat} , is that it uses only a partial MMD loss function when computing each gradient step in the optimization. For a detailed summary of the training procedure, see Algorithm A.1 in Appendix A.

3 Probabilistic forecasts and out-of-sample assessments

We now describe how to make rolling probabilistic forecasts from our estimated MTS model by simulating multiple sample paths forward and constructing *empirical predictive distributions* at each time point. Furthermore, we address how to assess these forecasts with out-of-sample test data. Specifically, we consider a *test period* consisting of time points $\tau + 1, \tau + 2, \dots, T$.

3.1 Rolling probabilistic forecasts

Let $h \in \{1, \dots, T - \tau\}$ denote the simulation horizon. For every $t = \tau, \dots, T - h$, once all realizations up to and including time t — namely, $(\mathbf{X}_s)_{s \leq t}$ — become available, we can simulate n_{pth} -many h -step ahead sample paths conditional on this past information $\mathcal{F}_t = \sigma(\{\mathbf{X}_s : s \leq t\})$. Let

$$\hat{X}_{n_{\text{pth}}, h | \mathcal{F}_t} = \{\hat{\mathbf{X}}_{t+1}^{(i)}, \hat{\mathbf{X}}_{t+2}^{(i)}, \dots, \hat{\mathbf{X}}_{t+h}^{(i)} | \mathcal{F}_t\}_{i=1}^{n_{\text{pth}}}$$

denote such sample paths, encoding an *empirical predictive distribution* at each time point $t + 1, t + 2, \dots, t + h$, from which various probabilistic forecasts can be made — for example, we can forecast $\mathbb{P}(\mathbf{X}_{t+2} > x)$ by $(1/n_{\text{pth}}) \sum_{i=1}^{n_{\text{pth}}} I(\hat{\mathbf{X}}_{t+2}^{(i)} > x)$.

Figure 1 provides a schematic illustration of what time periods are used respectively for training and testing, as well as how rolling probabilistic forecasts are made as we move forward step by step in time. In particular, we use the realizations $\mathbf{X}_1, \dots, \mathbf{X}_\tau$ to train our MTS model and the realizations $\mathbf{X}_{\tau+1}, \dots, \mathbf{X}_T$ to evaluate the rolling probabilistic forecasts made from our trained MTS model. At each particular time point $t = \tau, \dots, T - h$, we use all available realizations up to and including time t , that is, \mathcal{F}_t , to construct h -step ahead probabilistic forecasts $\hat{X}_{n_{\text{pth}}, h | \mathcal{F}_t}$, but we do not re-fit the MTS model itself.

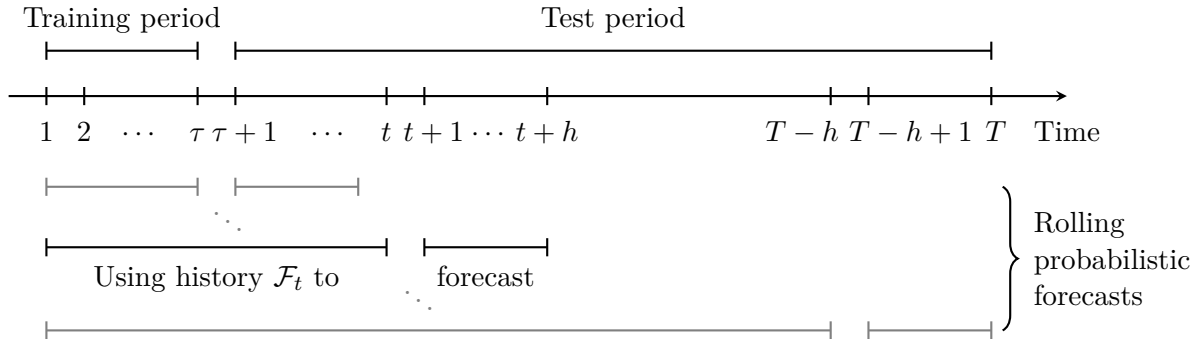


Figure 1 Time periods used for training, testing and the rolling probabilistic forecasts. At each time point $t = \tau, \dots, T - h$, the available history \mathcal{F}_t is used to make an h -step ahead probabilistic forecast $\hat{X}_{n_{\text{pth}}, h | \mathcal{F}_t}$.

A key component for simulating the paths is the generation of samples from the estimated dependence model. For fitted parametric copulas \hat{C}_{PM} , one typically uses a model-specific stochastic representation

to sample \mathbf{U}_t ; see, e.g., Hofert, Kojadinovic, et al. (2018, Chapter 3). For obtaining samples from the standard empirical copula, we can simply resample with replacement from $\hat{\mathbf{U}}_1, \dots, \hat{\mathbf{U}}_\tau$. For the empirical beta copula, we instead resample with replacement from a collection of uniform order statistics that are indexed by the ranks $R_{t,j}$, $t = 1, \dots, \tau$, $j = 1, \dots, d^*$; see Segers et al. (2017) for details. Sampling from the fitted GMMN $f_{\hat{\theta}}$ (with corresponding empirical copula \hat{C}_{NN}) can be done as follows.

Algorithm 3.1 (GMMN sampling)

- 1) Fix the number n_{gen} of samples to generate from \hat{C}_{NN} .
- 2) Draw $\mathbf{V}_1, \dots, \mathbf{V}_{n_{\text{gen}}} \stackrel{\text{ind.}}{\sim} F_{\mathbf{V}}$ from the prior distribution.
- 3) Return the pseudo-observations of $\mathbf{U}_s = f_{\hat{\theta}}(\mathbf{V}_s)$, $s = 1, \dots, n_{\text{gen}}$.

At any particular time point $t = \tau, \dots, T - h$, we can now utilize Algorithm 3.1 along with the fitted marginal time series models in our framework in order to simulate paths $\hat{X}_{n_{\text{pth}}, h | \mathcal{F}_t}$ with a fixed horizon h , as outlined in Algorithm 3.2.

Algorithm 3.2 (Rolling probabilistic forecasts from a GMMN–GARCH model without re-fitting)

- 1) Fix the number of sample paths n_{pth} and the simulation horizon h .
- 2) For $t = \tau, \dots, T - h$ do:
 - 2.1) Generate $\mathbf{U}_s^{(i)}$, $i = 1, \dots, n_{\text{pth}}$, $s = t + 1, \dots, t + h$, from the fitted GMMN \hat{C}_{NN} via Algorithm 3.1.
 - 2.2) For every $\mathbf{U}_s^{(i)}$ in Step 2.1), construct $\mathbf{Y}_s^{(i)} = (\hat{F}_1^{-1}(U_{s,1}^{(i)}), \dots, \hat{F}_{d^*}^{-1}(U_{s,d^*}^{(i)}))$. If no dimension reduction is utilized, \hat{F}_j^{-1} , $j = 1, \dots, d^*$, are the quantile functions of the fitted parametric innovation distributions selected as part of the ARMA–GARCH model setup; otherwise, they are the empirical quantile functions of $\hat{Y}_{1,j}, \dots, \hat{Y}_{\tau,j}$, $j = 1, \dots, d^*$.
 - 2.3) For every $\mathbf{Y}_s^{(i)}$ in Step 2.2), construct samples from the fitted innovation distributions via the transform $\mathbf{Z}_s^{(i)} = \hat{\mathbf{\Gamma}} \mathbf{Y}_s^{(i)}$; note that $\mathbf{Y}_s^{(i)} \in \mathbb{R}^{d^*}$ whereas $\mathbf{Z}_s^{(i)} \in \mathbb{R}^d$.
 - 2.4) For each $j = 1, \dots, d$, compute $\hat{\sigma}_{s,j}^{2(i)}$, $\hat{\mu}_{s,j}^{(i)}$ and $\hat{X}_{s,j}^{(i)}$, for $i = 1, \dots, n_{\text{pth}}$ and $s = t + 1, \dots, t + h$, via

$$\begin{aligned} \hat{\mu}_{s,j}^{(i)} &= \hat{\mu}_j + \sum_{k=1}^{\hat{p}_{1j}} \hat{\phi}_{jk} (\hat{X}_{s-k,j}^{(i)} - \hat{\mu}_j) + \sum_{l=1}^{\hat{q}_{1j}} \hat{\gamma}_{jl} (\hat{X}_{s-l,j}^{(i)} - \hat{\mu}_{s-l,j}^{(i)}), \\ \hat{\sigma}_{s,j}^{2(i)} &= \hat{\omega}_j + \sum_{k=1}^{\hat{p}_{2j}} \hat{\alpha}_{jk} (\hat{X}_{s-k,j}^{(i)} - \hat{\mu}_{s-k,j}^{(i)})^2 + \sum_{l=1}^{\hat{q}_{2j}} \hat{\beta}_{jl} \hat{\sigma}_{s-l,j}^{2(i)}, \\ \hat{X}_{s,j}^{(i)} &= \hat{\mu}_{s,j}^{(i)} + \hat{\sigma}_{s,j}^{2(i)} Z_{s,j}^{(i)}, \end{aligned}$$
 where, for $s \leq t$, set $\hat{X}_{s,j}^{(i)} = X_{s,j}$, $\hat{\sigma}_{s,j}^{2(i)} = \hat{\sigma}_{s,j}^2$, and $\hat{\mu}_{s,j}^{(i)} = \hat{\mu}_{s,j}$ for all $i = 1, \dots, n_{\text{pth}}$.
- 2.5) Return $\hat{\mathbf{X}}_s^{(i)} = (\hat{X}_{s,1}^{(i)}, \dots, \hat{X}_{s,d}^{(i)})$, $i = 1, \dots, n_{\text{pth}}$, $s = t + 1, \dots, t + h$.

Note that Step 2.1) in Algorithm 3.2 can be replaced by sampling from a fitted parametric copula \hat{C}_{PM} or nonparametric copula \hat{C}_{NPM} to obtain the classical approach for sampling paths in the copula–GARCH framework.

While Algorithm 3.2 describes how to simulate paths $\hat{X}_{n_{\text{pth}}, h | \mathcal{F}_t}$ for any simulation horizon h , we will focus on one-step ahead ($h = 1$) empirical predictive distributions henceforth.

3.2 Out-of-sample assessments

We assess two different aspects of out-of-sample performance with data in the test period; again, see Figure 1. We are interested in the following questions. First, how well has the cross-sectional dependence structure been captured? Second, how good are the resulting empirical predictive distributions?

3.2.1 Assessing the quality of the cross-sectional dependence model in the test period

We can use the MMD statistic to measure how close the empirical distributions of a fitted GMMN \hat{C}_{NN} , a fitted parametric copula \hat{C}_{PM} and a nonparametric copula \hat{C}_{NPM} match the cross-sectional dependence structure of the test dataset, $\mathbf{X}_{\tau+1}, \dots, \mathbf{X}_T$. This cross-sectional dependence structure can be extracted using the fitted (marginal) ARMA–GARCH models and the fitted PCA model (if dimension reduction is applied), as described in the following algorithm.

Algorithm 3.3 (Extracting the dependence structure of the test dataset)

- 1) Compute $\hat{\sigma}_{t,j}^2$, $\hat{\mu}_{t,j}$ and $\hat{Z}_{t,j}$ for $t = \tau + 1, \dots, T$ and $j = 1, \dots, d$ via

$$\begin{aligned}\hat{\mu}_{t,j} &= \hat{\mu}_j + \sum_{k=1}^{\hat{p}_{1j}} \hat{\phi}_{jk}(X_{t-k,j} - \hat{\mu}_j) + \sum_{l=1}^{\hat{q}_{1j}} \hat{\gamma}_{jl}(X_{t-l,j} - \hat{\mu}_{t-l,j}), \\ \hat{\sigma}_{t,j}^2 &= \hat{\omega}_j + \sum_{k=1}^{\hat{p}_{2j}} \hat{\alpha}_{jk}(X_{t-k,j} - \hat{\mu}_{t-k,j})^2 + \sum_{l=1}^{\hat{q}_{2j}} \hat{\beta}_{jl}\hat{\sigma}_{t-l,j}^2, \\ \hat{Z}_{t,j} &= \frac{X_{t,j} - \hat{\mu}_{t,j}}{\hat{\sigma}_{t,j}}.\end{aligned}$$

- 2) Obtain a sample from the underlying empirical stationary distribution via the transform $\hat{\mathbf{Y}}_t = \hat{\mathbf{\Upsilon}}^\top \hat{\mathbf{Z}}_t$, $t = \tau + 1, \dots, T$. (Note that $\hat{\mathbf{Z}}_t \in \mathbb{R}^d$ whereas $\hat{\mathbf{Y}}_t \in \mathbb{R}^{d^*}$.)
- 3) Return the pseudo-observations $\hat{\mathbf{U}}_t = (\hat{U}_{t,1}, \dots, \hat{U}_{t,d^*})$ of $\hat{\mathbf{Y}}_t$, for $t = \tau + 1, \dots, T$.

Let $\hat{\mathbf{U}} = (\hat{\mathbf{U}}_{\tau+1}^\top, \dots, \hat{\mathbf{U}}_T^\top)^\top \in [0, 1]^{(T-\tau) \times d^*}$ denote the pseudo-observations obtained from the test dataset via Algorithm 3.3. Furthermore, let $\mathbf{U} = (\mathbf{U}_1^\top, \dots, \mathbf{U}_{n_{\text{gen}}}^\top)^\top \in [0, 1]^{n_{\text{gen}} \times d^*}$ denote a sample generated from either \hat{C}_{NN} , \hat{C}_{PM} or \hat{C}_{NPM} , where we choose $n_{\text{gen}} = T - \tau$ (other choices are possible). We can then compute one realization of the MMD statistic $\text{MMD}(\hat{\mathbf{U}}, \mathbf{U}; K)$ as in (1). In our analysis in Section 4, we then use an average MMD statistic based on n_{rep} repeated samples $\mathbf{U}^{(i)} \in [0, 1]^{n_{\text{gen}} \times d^*}$, $i = 1, \dots, n_{\text{rep}}$, given by

$$\text{AMMD} = \frac{1}{n_{\text{rep}}} \sum_{i=1}^{n_{\text{rep}}} \text{MMD}(\hat{\mathbf{U}}, \mathbf{U}^{(i)}; K_{\text{tst}}). \quad (4)$$

Remark 3.4

Here, we would like to emphasize that, even though the GMMNs are trained to optimize the MMD statistic on the training dataset, the AMMD metric defined in (4) is still a fair out-of-sample assessment metric since

- 1) it is applied to compare GMMN-generated samples $\mathbf{U}^{(i)}$ against realized innovation copula-samples $\hat{\mathbf{U}}$ from the *test dataset*, not the training dataset; and
- 2) $K_{\text{tst}} \neq K_{\text{trn}}$, so a *different* mixture of Gaussian kernels is used for the assessment than the one used for training the GMMN.

3.2.2 Assessing the quality of empirical predictive distributions

While there exist numerous metrics to assess univariate or multivariate point forecasts, there are only a handful of metrics that can be used to evaluate the quality of dependent multivariate empirical predictive distributions. We now present two such metrics we will use across all numerical examples.

Firstly, we use a version of the *mean squared error (MSE)* metric defined via the Euclidean norm to assess how well the empirical predictive distribution $\hat{X}_{n_{\text{pth}},1|\mathcal{F}_{t-1}}$ concentrates around each true value \mathbf{X}_t in the test dataset, so for $t = \tau + 1, \dots, T$. To obtain a single numerical value, we work with an average MSE metric computed over the entire test period $t = \tau + 1, \dots, T$, defined by

$$\text{AMSE} = \frac{1}{T - \tau} \sum_{t=\tau+1}^T \frac{1}{n_{\text{pth}}} \sum_{i=1}^{n_{\text{pth}}} \|\hat{\mathbf{X}}_t^{(i)} - \mathbf{X}_t\|_2^2. \quad (5)$$

Secondly, we use the *variogram score* introduced by Scheuerer and Hamill (2015), which, in our context, assesses if the empirical predictive distribution is biased for the distance between any two component samples. For a single numeric summary, we work with an average variogram score (of order r) over the entire test period $t = \tau + 1, \dots, T$,

$$\text{AVS}^r = \frac{1}{T - \tau} \sum_{t=\tau+1}^T \sum_{j_1=1}^d \sum_{j_2=1}^d \left(|X_{t,j_1} - X_{t,j_2}|^r - \frac{1}{n_{\text{pth}}} \sum_{i=1}^{n_{\text{pth}}} |\hat{X}_{t,j_1}^{(i)} - \hat{X}_{t,j_2}^{(i)}|^r \right)^2. \quad (6)$$

As numerically demonstrated by Scheuerer and Hamill (2015), by focusing on pairwise distances between component samples, this metric discriminates well between various dependence structures.

4 Applications

In this section, we demonstrate the flexibility of our GMMN–GARCH approach when compared to the copula–GARCH approach. To that end, we focus on modeling multivariate yield curve and exchange-rate time series. Before delving into the two financial econometrics applications, we will first detail the selection and setup of component models within our framework that will be utilized for all examples in this section. Specifically, we will describe the choice of marginal time series models, the implementation details for GMMN models, and the choice of parametric and nonparametric copula models used for comparison. All examples in this section were implemented in R. GMMN models were fitted with the package `gmn`, while various other R packages (see below) were used to fit ARMA–GARCH models, parametric and nonparametric copula models, and so on. The R packages `keras` and `tensorflow` were used as R interfaces to the corresponding namesake Python libraries. All GMMN training was carried out on a single NVIDIA Tesla P100 GPU with 12 GB RAM; see Hofert, Prasad, et al. (2021, Appendix B) for various aspects on run time measurements. While we convey our results through plots in this section, we also report them in the form of tables in Appendix B.

4.1 Multivariate time series modeling: setup and implementation details

4.1.1 Serial dependence models

For modeling the marginal time series, we take the broad-brush approach and choose to fit ARMA(1,1)–GARCH(1,1) models with scaled t innovation distributions $F_j(z_j) = t_{\nu_j}(z_j \sqrt{\nu_j/(\nu_j - 2)})$, $j = 1, \dots, d$, to each component sample. As mentioned earlier, these models are popular choices for modeling univariate financial time series. To fit them, we use the function `fit_ARMA_GARCH(, solver =`

"hybrid") from the R package `qrmtools` which relies on `ugarchfit()` from the R package `rugarch` (see Ghalanos (2019)).

4.1.2 Cross-sectional dependence models: GMMN architecture and training setup

In both applications, we experiment with five NN architectures containing a different number of hidden layers and neurons per layer. For a NN with single hidden layer, we consider three architectures with 100 ($\text{NN}_{100}^{1\times}$), 300 ($\text{NN}_{300}^{1\times}$) and 600 ($\text{NN}_{600}^{1\times}$) neurons per layer, respectively. While we generally find that the single-hidden-layer architecture provides sufficient flexibility for the applications under consideration, we also consider two deeper NN architectures for the sake of comparison. Due to increased computational complexity with each added hidden layer, we consider a wide two-hidden-layer architecture with 600 neurons per layer ($\text{NN}_{600}^{2\times}$) and a narrower three-hidden-layer architecture with only 300 neurons per layer ($\text{NN}_{300}^{3\times}$). We fix the activation function in each hidden layer to be ReLU since it offers computational efficiency via non-expensive and non-vanishing gradients, and the activation function in the output layer to be sigmoid since our target output lies in $[0, 1]^{d^*}$. Additionally, we use batch normalization and dropout regularization (with a dropout rate of 0.5) in the hidden layers to facilitate the training of these five NNs while also controlling for overfitting.

As mentioned earlier in Section 2.3.3, we utilize a mixture of Gaussian kernels K_{trn} to compute the MMD statistic defined in (1) when training. To this end, we fix $n_{\text{krn}} = 6$ and choose bandwidth parameters $(\sigma_1, \dots, \sigma_6) = (0.001, 0.01, 0.15, 0.25, 0.50, 0.75)$ as done in Hofert, Prasad, et al. (2021). This hyperparameter setting is specifically suited for copula samples or pseudo-observations as they lie in $[0, 1]^{d^*}$. Furthermore, it was demonstrated in Hofert, Prasad, et al. (2021) that GMMNs trained with this particular specification of the loss function were capable of learning a wide variety of complex dependence structures.

We choose the dimension of the prior distribution F_V to be $p = d^*$. As a result we obtain a natural d^* -to- d^* GMMN transform f_θ . Following common practice, we select $\mathbf{V} \sim \mathcal{N}(\mathbf{0}, I_{d^*})$, where I_{d^*} denotes the identity matrix in $\mathbb{R}^{d^* \times d^*}$. Hence \mathbf{V} consists of independent standard normal random variables. Since we are working with a modest number of training data points in each of the datasets considered, we opt for a batch optimization procedure presented as a special case ($n_{\text{bat}} = \tau$) of Algorithm A.1. For the number of epochs, we choose $n_{\text{epo}} = 1000$ which ensures a sufficiently long training period to obtain accurate results.

4.1.3 Cross-sectional dependence models: parametric copulas

For a comparison with GMMN-GARCH models, we also present results for a number of different parametric copula models C_{PM} . These include Gumbel copulas, normal copulas with exchangeable correlation matrices, t copulas with exchangeable and with unstructured correlation matrices and vine copulas. For all copulas except vines, we use maximum pseudo-likelihood estimation via the function `fitCopula(, method = "mpl")` from the R package `copula`. We can then generate samples from the fitted copulas via `rCopula()`. For vine copulas, we use the `RvineStructureSelect()` function from the R package `VineCopula` to fit a regular-vine (R-vine) copula, where the tree structure is selected using Dissmann's algorithm (Dissmann et al. 2013) and the pair-copula families are selected using the AIC criteria. All parametric pair-copula families implemented in the R package `VineCopula` are considered when fitting the R-vine copula. We also produce results for the independence copula which serves as a simple benchmark model.

4.1.4 Cross-sectional dependence models: nonparametric copulas

Additionally, we compare GMMN–GARCH models with certain nonparametric copula models. The latter include the standard empirical copula and the smoothed empirical beta copula estimators. We use the `empCopula()` and `rCopula()` functions from the R package `copula` to fit and simulate from these two types of empirical copulas.

4.2 Yield curve modeling

Analyzing and modeling *zero-coupon bond (ZCB) yield curves*, also referred to as the *term structure of interest rates*, is a critical task in various financial and economic applications. While early research in this area is often solely focused on constructing models of yield curves based on economic theory, the seminal work by Diebold and Li (2006) focused on the critical task of yield curve forecasting.

The primary approach showcased in Diebold and Li (2006) was the embedding of autoregressive models within the parametric structure of the three factor Nelson–Siegel model (Nelson and Siegel 1987) which intuitively characterizes the level, slope and curvature of the yield curve. Since then various approaches for forecasting yield curves have been investigated; see Diebold and Rudebusch (2013) for an overview and Caldeira et al. (2016) for a recently proposed forecast combination approach. Most models proposed and reviewed in the literature are particularly designed towards constructing point forecasts for yield curves. Such point forecasts are typically useful in bond portfolio optimization and in the pricing of certain financial assets. Alternatively, distributional forecasts of ZCB yield curves could potentially be helpful in risk management applications, derivative pricing (via simulation) and economic scenario generation. To that end, in this section, we consider modeling US and Canadian ZCB yield curves using MTS models. We then utilize our fitted GMMN–GARCH models to obtain empirical predictive distributions of these ZCB yield curves.

4.2.1 Modeling US and Canadian ZCB data

For US treasury ZCB data, we consider a 30-dimensional yield curve constructed from ZCBs with times to maturity ranging from 1 to 30 years in annual increments. For Canadian ZCB data, we consider a 120-dimensional yield curve constructed from ZCBs with times to maturity ranging from 0.25 to 30 years in quarterly increments. Refer to the R package `qrmdata` for further details about these data. In particular, we consider these multivariate time series in the time period from 1995-01-01 to 2015-12-31 (2015-08-31 for the Canadian data), treating data from 1995-01-01 to 2014-12-31 as the training set and the remainder as the test dataset.

As a pre-processing step, we begin by applying a simple difference transform to the original time series. We then take the transformed series to be the series \mathbf{X}_t that we work with.

Following our framework, we first model the marginal time series using the ARMA–GARCH model setup described in Section 4.1.1 with $\mu_j = 0$, $j = 1, \dots, d$. Since these data are relatively high-dimensional ($d = 30$ for the US data and $d = 120$ for the Canadian data), we apply PCA to the standardized residuals $\hat{\mathbf{Z}}_t$ for dimension reduction. Yield curves are indeed amenable to good approximations via lower dimensional representations; various dimension reduction techniques such as factor models have been incorporated by various yield curve models (see, e.g., Diebold and Li 2006). We choose the number of top principal components k to construct the lower dimensional representation for each dataset as follows. We select the smallest $k \geq 3$ such that the first k principal components account for at least 95% of the total variance in the standardized residuals $\hat{\mathbf{Z}}_t$. For the US data, this choice is $k = 3$; for the Canadian data, it is $k = 4$.

4.2.2 Assessment

We evaluate the performance of our models on the test dataset using the metrics discussed in Section 3.2. First, we compute the AMMD metric (4) using $n_{\text{rep}} = 100$ replications to assess the quality of the dependence models in the test period; see the explanations in Remark 3.4 for why the AMMD metric is a fair out-of-sample assessment metric. For the Gaussian mixture kernel K_{tst} in (4), we fix $n_{\text{knn}} = 5$ and select the bandwidth parameters $\sigma = (0.1, 0.3, 0.5, 0.7, 0.9)$. Then, to assess if capturing the underlying cross-sectional dependence structure well translates to better one-day-ahead empirical predictive distributions, we compute the AMSE metric (5) and the AVS^r metric (6) using $n_{\text{pth}} = 1000$ simulated paths. For the average variogram score metric AVS^r , a typical choice for the order may be $r = 0.5$ as stated in Scheuerer and Hamill (2015). However, since their concluding remarks note that smaller values of r could potentially yield more discriminative metrics when dealing with non-Gaussian data, we choose $r = 0.25$.

Figure 2 displays scatter plots of AMSE (left) and $\text{AVS}^{0.25}$ (right) versus AMMD for the US (top) and Canadian (bottom) data. For both datasets, samples generated from the five GMMN models (see Section 4.1.2) more closely match the underlying cross-sectional dependence structure in their corresponding test datasets than those generated from the five parametric copulas, the independence copula (see Section 4.1.3) and the two nonparametric copulas (see Section 4.1.4). Moreover, across the entire spectrum of GMMN–GARCH and copula–GARCH models being studied, it is also clear that better dependence modeling (as measured by the AMMD metric) does typically translate into better one-day-ahead empirical predictive distributions (as measured by the AMSE and $\text{AVS}^{0.25}$ metrics). Specifically, almost all GMMN models (with very few exceptions) clearly outperform the best parametric copula model (that is, typically either an R-vine copula or a t -copula with unstructured correlation matrix) and the two types of nonparametric copulas in all three metrics — although among the GMMN models themselves there is not a single best one. Note that more complicated NN architectures ($\text{NN}_{600}^{2\times}$ and $\text{NN}_{300}^{3\times}$) do not necessarily yield better dependence models and (hence) better empirical predictive distributions with respect to the considered metrics.

4.3 Exchange-rate modeling

The modeling and analysis of foreign exchange-rate dependence is an important task in risk management applications involving a global portfolio of financial assets. As such, dependent multivariate time series of exchange rates have been previously studied in the copula literature; see, e.g., Patton (2006) or Dias and Embrechts (2010). In this section, we consider modeling foreign exchange-rate data with respect to the US dollar (USD) and Pound sterling (GBP) using MTS models. We then utilize our fitted GMMN–GARCH and copula–GARCH models to obtain empirical predictive distributions and Value-at-Risk (VaR) forecasts for portfolios of exchange-rate assets.

4.3.1 Modeling USD and GBP exchange-rate data

For the USD exchange-rate data, we consider the daily exchange rates of Canadian dollar (CAD), Pound sterling (GBP), Euro (EUR), Swiss Franc (CHF) and Japanese yen (JPY) with respect to the USD. For the GBP exchange-rate data, we consider the daily exchange rates of CAD, USD, EUR, CHF, JPY and the Chinese Yuan (CNY) with respect to the GBP. For further details regarding both the USD and GBP exchange-rate data, see the R package `qrmdata`. In particular, we consider these multivariate time series in the time period from 2000-01-01 to 2015-12-31, treating data up to 2014-12-31 as the training set and the remainder as the test dataset. Due to the fixed peg of the CNY against the USD, particularly prior to August 2005, we do not include it in the USD dataset.

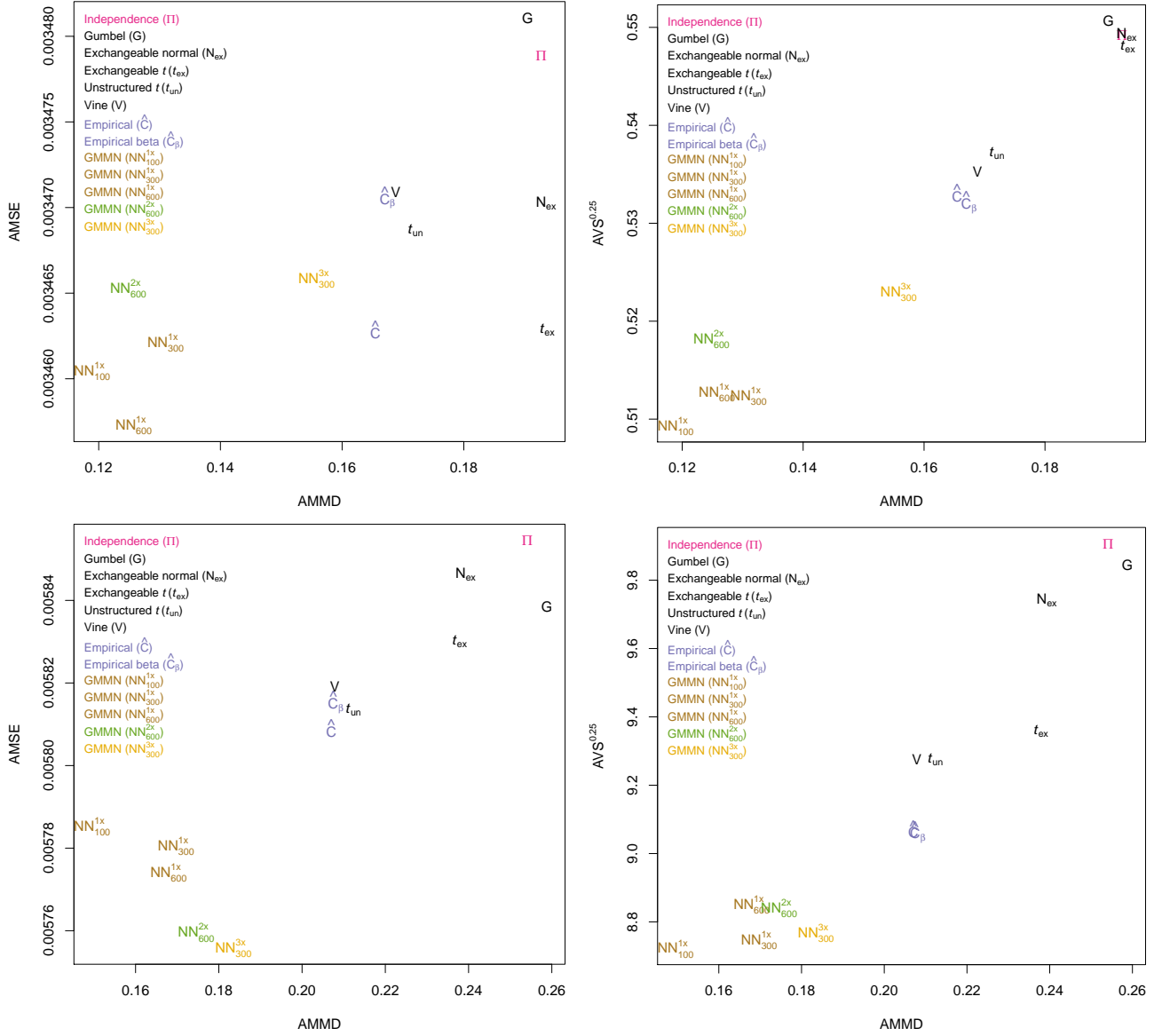


Figure 2 Model assessments for US (top) and Canadian (bottom) ZCB yield curve data. Scatter plots of AMSE (left) and $AVS^{0.25}$ (right) computed based on $n_{\text{pth}} = 1000$ simulated paths versus AMMD computed based on $n_{\text{rep}} = 100$ realizations. All models incorporate PCA with $k = 3$ (US) and $k = 4$ (Canadian) principal components.

To begin with, we apply the log-returns transformation to the nominal exchange rates and work with the resulting return series for modeling. Following our framework, we start by modeling the marginal time series using the ARMA–GARCH specification as detailed in Section 4.1.1. Since these datasets are relatively low-dimensional ($d = 5$ for the USD data and $d = 6$ for the GBP data), we do not incorporate any dimension reduction step in this analysis.

4.3.2 Assessment

Following the setup in Section 4.2.2, we evaluate the performance of our models with the AMMD, AMSE and $AVS^{0.25}$ metrics on the test dataset. Figure 3 displays scatter plots of AMSE (left) and $AVS^{0.25}$ (right) versus AMMD for the USD (top) and GBP (bottom) data. We can draw the same conclusions from this figure as those from Figure 2. In addition, here we also observe that the independence copula performs noticeably worse than all other models, whether capturing the dependence structure of the innovation distribution or making probabilistic forecasts.

4.3.3 Forecasting daily portfolio VaR

As demonstrated in the previous section, GMMN–GARCH models produce better one-day-ahead empirical predictive distributions when compared with various copula–GARCH models. We can utilize these one-day-ahead empirical predictive distributions to extract forecasts of various quantities of interest in risk management. One such popular quantity is the Value-at-Risk (VaR) of a portfolio.

To begin with, consider the aggregate return $S_t = \sum_{j=1}^d X_{t,j}$ at time t . Then, the (theoretical) VaR at confidence level α and time t is given by $\text{VaR}_\alpha(S_t) = F_{S_t}^{-1}(\alpha)$ where $F_{S_t}^{-1}$ denotes the quantile function of S_t . In practice, we can compute the empirical α -quantile of S_t from its empirical predictive distribution, $\{\hat{S}_t^{(i)} = \sum_{j=1}^d \hat{X}_{t,j}^{(i)} \mid \mathcal{F}_{t-1}\}_{i=1}^{n_{\text{pth}}}$. We denote the corresponding forecast by $\widehat{\text{VaR}}_\alpha(\hat{S}_t)$. Thus, for each MTS model, we compute daily forecasts $\widehat{\text{VaR}}_\alpha(\hat{S}_t)$ for every $t = \tau + 1, \dots, T$ in the test period. To assess the quality of these forecasts, we can compute the frequency with which S_t actually exceeds the daily forecast $\widehat{\text{VaR}}_\alpha(\hat{S}_t)$ over the entire test period. We expect this frequency to be α . Hence, we can evaluate our VaR forecasts by measuring the (absolute) error between the actual and the expected exceedance frequency, or simply the *VaR exceedance absolute error*, defined by

$$\text{VEAR}_\alpha = \left| \alpha - \frac{1}{T - \tau} \sum_{t=\tau+1}^T \mathbb{1}_{\{S_t < \widehat{\text{VaR}}_\alpha(\hat{S}_t)\}} \right|. \quad (7)$$

Figure 4 displays scatter plots of $\text{VEAR}_{0.05}$ versus AMMD for the USD (left) and GBP (right) exchange-rate data. For both datasets, the GMMN–GARCH models typically produce better daily VaR forecasts of $\text{VaR}_{0.05}(S_t)$ than the five parametric and two nonparametric copula–GARCH models do. Particularly, assuming independence among the exchange-rate returns leads to notably poorer forecasts. However, as expected it is slightly more difficult to discriminate between the various forecasts when the evaluation metric is based on a specific α -quantile of the empirical predictive distribution of the aggregated returns as opposed to the entire multivariate empirical predictive distribution.

5 Conclusion

We introduced generative moment matching networks (GMMNs) for modeling the dependence in MTS data. First, ARMA–GARCH models are used to marginally model serial dependence. Second, for high-dimensional MTS data, a dimension reduction method can be applied. Last, the cross-sectional

5 Conclusion

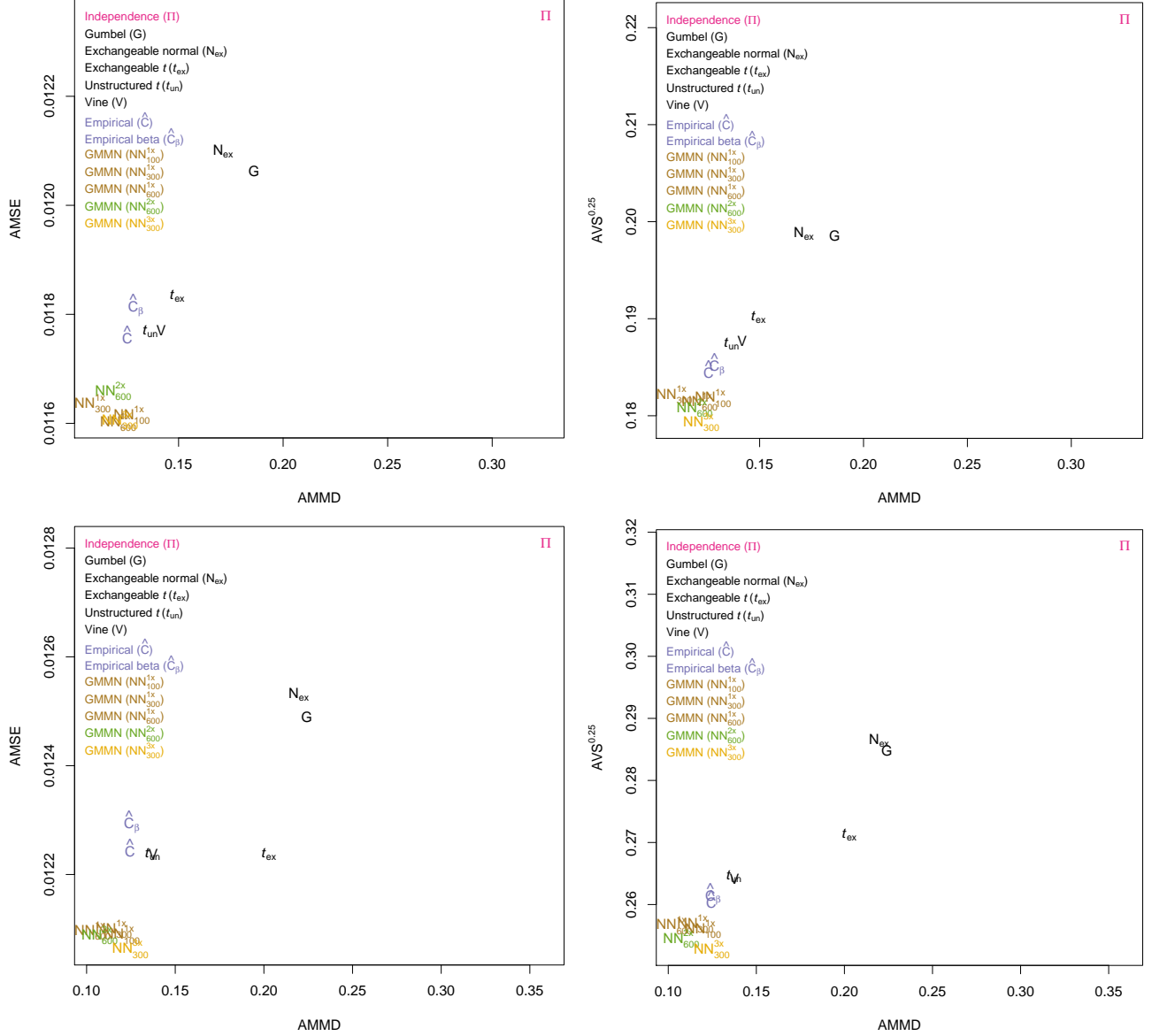


Figure 3 Model assessments for USD (top) and GBP (bottom) exchange-rate data. Scatter plots of AMSE (left) and AVS^{0.25} (right) computed based on $n_{pth} = 1000$ simulated paths versus AMMD computed based on $n_{rep} = 100$ realizations.

5 Conclusion

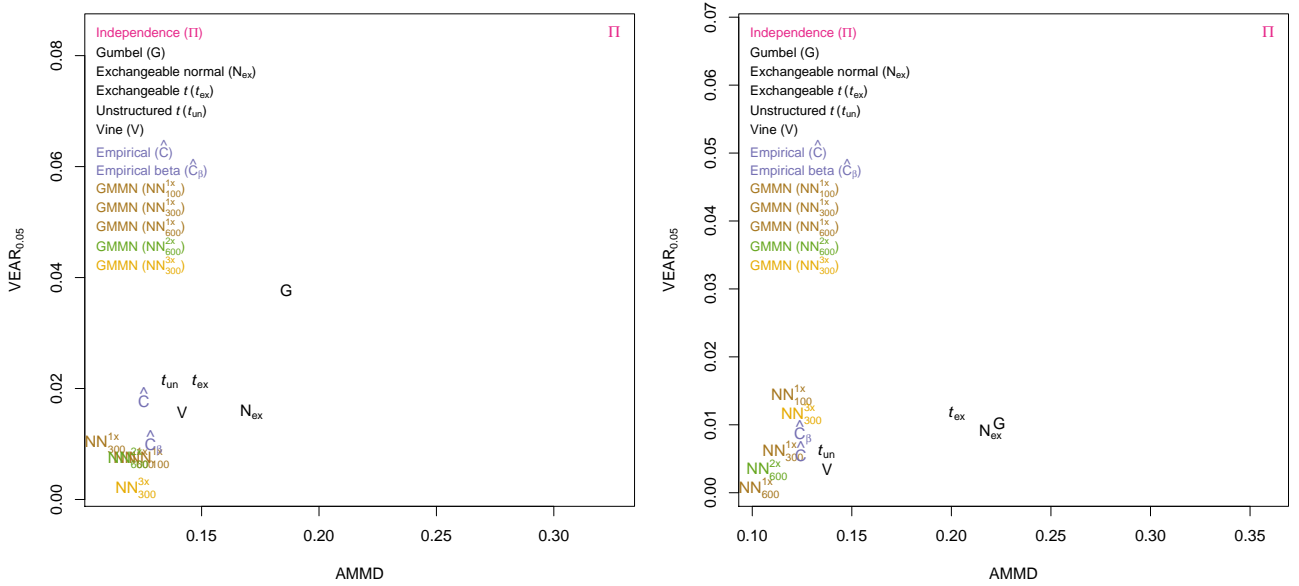


Figure 4 VaR forecast assessments for USD (left) and GBP (right) exchange-rate data. Scatter plots of $\text{VaR}_{0.05}$ computed based on $n_{\text{pth}} = 1000$ simulated paths versus AMMD computed based on $n_{\text{rep}} = 100$ realizations.

dependence is modeled by a GMMN. In the popular copula–GARCH approach, the latter step typically requires us to find a parametric copula model which fits the given data well. This can already be a challenging task in moderately large dimensions. By contrast, GMMNs are highly flexible and easy to simulate from, which is a major advantage of our GMMN–GARCH approach. The primary objective of fitting these MTS models is to produce empirical predictive distributions, with which we can then forecast various quantities of interest in risk management such as VaR or expected shortfall.

To showcase the flexibility of our GMMN–GARCH framework, we considered modeling ZCB yield curves and foreign exchange-rate returns. Across all the examples considered, we demonstrated that fairly simple GMMNs were able to better capture the underlying cross-sectional dependence than many well-known parametric and nonparametric copulas. Consequentially, we observed that the corresponding GMMN–GARCH models yielded superior one-step ahead empirical predictive distributions. Additionally, for exchange-rate data, we demonstrated that GMMN–GARCH models produced more accurate daily portfolio VaR forecasts as well.

For the first two modeling steps in our framework, we used ARMA–GARCH models and principal component analysis. However, a variety of other models can be applied here as long as iid data results as residuals which can then be used to train GMMNs. A potential avenue for future research involves constructing new and highly flexible MTS models by combining different types of marginal time series models and dimension reduction techniques with GMMNs. In particular, one would be interested in capturing different types of (marginal) temporal dependencies and leveraging more sophisticated dimension reduction techniques for constructing even better higher dimensional time series models.

As Hofert, Prasad, et al. (2021) showed, one advantage of GMMNs as dependence models is that one obtains, for free, a quasi-random number generator from the respective model. In how far the low discrepancy property propagates to a variance-reduction effect in forecasted quantities for dependent multivariate time series is also an interesting question of future research.

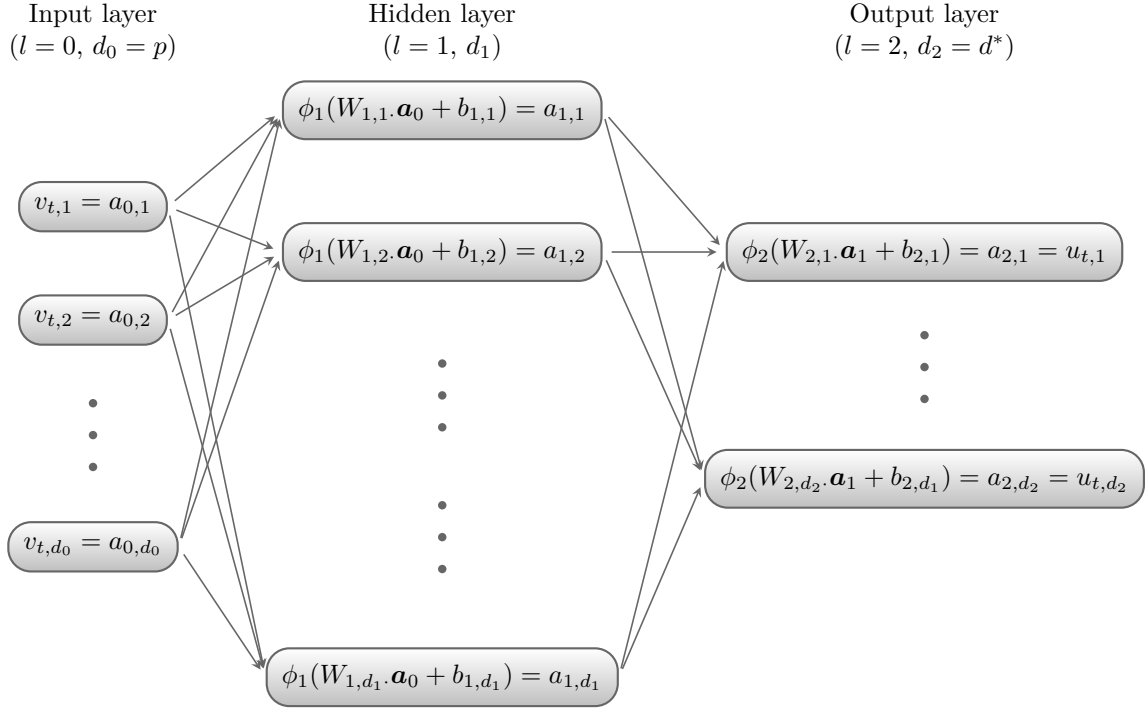


Figure 5 Structure of a NN with input $\mathbf{v}_t = (v_{t,1}, \dots, v_{t,d_0})$, $L = 1$ hidden layer with output $\mathbf{a}_1 = f_1(\mathbf{a}_0) = \phi_1(W_1 \mathbf{a}_0 + \mathbf{b}_1)$ and output layer with output $\mathbf{u}_t = \mathbf{a}_2 = f_2(\mathbf{a}_1) = \phi_2(W_2 \mathbf{a}_1 + \mathbf{b}_2)$; note that, $W_{l,j}$ denotes the j th row of W_l and $b_{l,j}$ the j th element of \mathbf{b}_l .

A GMMNs: Additional details

In this section, we provide some additional details pertaining to the NN architecture and GMMN training.

Feedforward neural networks

Let L be the number of hidden layers in the NN and, for each $l = 0, \dots, L + 1$, let d_l be the dimension of layer l , that is the number of neurons in layer l . Layer $l = 0$ refers to the *input layer* which consists of the input $\mathbf{v}_t \in \mathbb{R}^p$ for $d_0 = p$, and layer $l = L + 1$ refers to the *output layer* which consists of the output $\mathbf{u}_t \in [0, 1]^{d^*}$ for $d_{L+1} = d^*$. The *hidden* layers $l = 1, \dots, L + 1$ can be described in terms of the output $\mathbf{a}_{l-1} \in \mathbb{R}^{d_{l-1}}$ of layer $l - 1$ via

$$\begin{aligned} \mathbf{a}_0 &= \mathbf{v}_t \in \mathbb{R}^{d_0}, \\ \mathbf{a}_l &= f_l(\mathbf{a}_{l-1}) = \phi_l(W_l \mathbf{a}_{l-1} + \mathbf{b}_l) \in \mathbb{R}^{d_l}, \quad l = 1, \dots, L + 1, \\ \mathbf{u}_t &= \mathbf{a}_{L+1} \in \mathbb{R}^{d_{L+1}}, \end{aligned}$$

with *weight matrices* $W_l \in \mathbb{R}^{d_l \times d_{l-1}}$, *bias vectors* $\mathbf{b}_l \in \mathbb{R}^{d_l}$ and *activation functions* ϕ_l ; the latter are understood to be applied componentwise for vector inputs. Some commonly used activation functions include the *sigmoid* activation function $\phi_l(x) = 1/(1 + e^x)$ and the *rectified linear unit (ReLU)* activation function $\phi_l(x) = \max\{0, x\}$. The NN $f_\theta : \mathbb{R}^p \leftarrow [0, 1]^{d^*}$ can then be written as the

composition

$$f_{\theta} = f_{L+1} \circ f_L \circ \cdots \circ f_2 \circ f_1,$$

with its flattened parameter vector $\theta = (W_1, \dots, W_{L+1}, \mathbf{b}_1, \dots, \mathbf{b}_{L+1})$. Figure 5 visualizes this construction and the notation we use. GMMNs are such type of NNs which, for training (that is, the fitting of θ), utilize a specific loss function introduced next.

GMMN training

Algorithm A.1 describes in detail the training of the GMMN f_{θ} using a mini-batch optimization procedure.

Algorithm A.1 (Training GMMNs)

- 1) Fix the number n_{epo} of epochs and the sample size per batch (the so-called *batch size*) $1 \leq n_{\text{bat}} \leq \tau$, where n_{bat} is assumed to divide τ . Initialize the epoch counter $k = 0$ and the GMMN's parameter vector $\theta = \theta^{(0)}$; we follow Glorot and Bengio (2010) and initialize the components of $\theta^{(0)}$ as $W_l \sim \text{U}(-\sqrt{6/(d_l + d_{l-1})}, \sqrt{6/(d_l + d_{l-1})})^{d_l \times d_{l-1}}$ and $\mathbf{b}_l = \mathbf{0}$ for $l = 1, \dots, L + 1$.
- 2) Initialize the vectors $\mathbf{m}_1^{(0)} = \mathbf{0}$ and $\mathbf{m}_2^{(0)} = \mathbf{0}$, where $\mathbf{m}_1^{(0)}$ and $\mathbf{m}_2^{(0)}$ have the same dimension as the parameter vector θ . Following Kingma and Ba (2014), we fix the exponential decay rates $\beta_1 = 0.9$ and $\beta_2 = 0.999$, the step size $\alpha = 0.001$ and the smoothing constant $\varepsilon = 10^{-8}$.
- 3) For epoch $k = 1, \dots, n_{\text{epo}}$, do:
 - 3.1) Randomly partition the training sample $\hat{U}_1, \dots, \hat{U}_{\tau}$ and the prior distribution sample $\mathbf{V}_1, \dots, \mathbf{V}_{\tau}$ into corresponding τ/n_{bat} non-overlapping batches $\hat{U}_1^{(b)}, \dots, \hat{U}_{n_{\text{bat}}}^{(b)}$ and $\mathbf{V}_1^{(b)}, \dots, \mathbf{V}_{n_{\text{bat}}}^{(b)}$, $b = 1, \dots, \tau/n_{\text{bat}}$, of size n_{bat} each.
 - 3.2) For batch $b = 1, \dots, \tau/n_{\text{bat}}$, let $r = b + (k - 1)\tau/n_{\text{bat}}$ and do:
 - 3.2.1) Compute the GMMN output $\mathbf{U}_s^{(b)} = f_{\theta^{(r-1)}}(\mathbf{V}_s^{(b)})$, $s = 1, \dots, n_{\text{bat}}$.
 - 3.2.2) Compute the gradient $\nabla^{(r)} = \frac{\partial}{\partial \theta} \text{MMD}(\hat{U}^{(b)}, U^{(b)}; K_{\text{trn}})$ from the samples $\hat{U}^{(b)} = (\hat{U}_1^{(b)\top}, \dots, \hat{U}_{n_{\text{bat}}}^{(b)\top})^{\top}$ and $U^{(b)} = (\mathbf{U}_1^{(b)\top}, \dots, \mathbf{U}_{n_{\text{bat}}}^{(b)\top})^{\top}$ via automatic differentiation.
 - 3.2.3) Update $\mathbf{m}_1^{(r)} = \beta_1 \mathbf{m}_1^{(r-1)} + (1 - \beta_1) \nabla^{(r)}$ and compute the bias corrected version $\tilde{\mathbf{m}}_1^{(r)} = \mathbf{m}_1^{(r)} / (1 - \beta_1^r)$.
 - 3.2.4) Update $\mathbf{m}_2^{(r)} = \beta_2 \mathbf{m}_2^{(r-1)} + (1 - \beta_2) (\nabla^{(r)})^2$, where all operations are understood to be applied componentwise, and compute the bias corrected version $\tilde{\mathbf{m}}_2^{(r)} = \mathbf{m}_2^{(r)} / (1 - \beta_2^r)$.
 - 3.2.5) Update the parameter vector $\theta^{(r)} = \theta^{(r-1)} - \alpha \tilde{\mathbf{m}}_1^{(r)} / (\sqrt{\tilde{\mathbf{m}}_2^{(r)}} + \varepsilon)$, where all operations are understood to be applied componentwise.
- 4) Return $\hat{\theta} = \theta^{(n_{\text{epo}}(\tau/n_{\text{bat}}))}$; the fitted GMMN is then $f_{\hat{\theta}}$.

B Applications: Tables of empirical results

In this section, we display tables of empirical results for the applications discussed in Section 4. For five GMMN models, five parametric copulas, the independence copula and two nonparametric copulas, Table 1 presents their respective AMMD, AMSE and AVS^{0.25} metrics for the US and Canadian ZCB yield curve data, while Table 2 presents their respective AMMD, AMSE, AVS^{0.25} and VEAR_{0.05} metrics for the USD and GBP exchange-rate data.

Data set	Dependence model	AMMD	AMSE	AVS ^{0.25}
US ZCB	Independence	0.1927	3.479×10^{-3}	0.5492
	Gumbel	0.1905	3.481×10^{-3}	0.5507
	Exchangeable normal	0.1935	3.470×10^{-3}	0.5493
	Exchangeable t	0.1936	3.463×10^{-3}	0.5480
	Unstructured t	0.1720	3.469×10^{-3}	0.5372
	Vine	0.1688	3.471×10^{-3}	0.5353
	Empirical	0.1655	3.463×10^{-3}	0.5331
	Empirical beta	0.1674	3.471×10^{-3}	0.5322
	GMMN (NN ₁₀₀ ^{1x})	0.1189	3.460×10^{-3}	0.5093
	GMMN (NN ₃₀₀ ^{1x})	0.1310	3.462×10^{-3}	0.5123
	GMMN (NN ₆₀₀ ^{1x})	0.1257	3.457×10^{-3}	0.5128
	GMMN (NN ₆₀₀ ^{2x})	0.1249	3.465×10^{-3}	0.5182
	GMMN (NN ₃₀₀ ^{3x})	0.1558	3.466×10^{-3}	0.5230
CAD ZCB	Independence	0.2541	5.854×10^{-3}	9.907
	Gumbel	0.2588	5.839×10^{-3}	9.844
	Exchangeable normal	0.2393	5.846×10^{-3}	9.741
	Exchangeable t	0.2378	5.830×10^{-3}	9.359
	Unstructured t	0.2123	5.814×10^{-3}	9.275
	Vine	0.2079	5.819×10^{-3}	9.276
	Empirical	0.2070	5.809×10^{-3}	9.072
	Empirical beta	0.2081	5.815×10^{-3}	9.063
	GMMN (NN ₁₀₀ ^{1x})	0.1496	5.785×10^{-3}	8.722
	GMMN (NN ₃₀₀ ^{1x})	0.1697	5.781×10^{-3}	8.747
	GMMN (NN ₆₀₀ ^{1x})	0.1679	5.774×10^{-3}	8.850
	GMMN (NN ₆₀₀ ^{2x})	0.1746	5.760×10^{-3}	8.841
	GMMN (NN ₃₀₀ ^{3x})	0.1835	5.756×10^{-3}	8.767

Table 1 Model assessment metrics for US (top) and Canadian (bottom) ZCB yield curve data. The AMSE and AVS^{0.25} metrics are computed based on $n_{\text{pth}} = 1000$ simulated paths while the AMMD metric is computed based on $n_{\text{rep}} = 100$ realizations. All models incorporate PCA with $k = 3$ (US) and $k = 4$ (Canadian) principal components.

Data set	Dependence model	AMMD	AMSE	AVS ^{0.25}	VEAR _{0.05}
USD FX	Independence	0.3257	1.235×10^{-2}	0.2209	8.425×10^{-2}
	Gumbel	0.1860	1.206×10^{-2}	0.1986	3.767×10^{-2}
	Exchangeable normal	0.1713	1.210×10^{-2}	0.1988	1.575×10^{-2}
	Exchangeable t	0.1492	1.183×10^{-2}	0.1902	2.123×10^{-2}
	Unstructured t	0.1363	1.177×10^{-2}	0.1874	2.123×10^{-2}
	Vine	0.1416	1.177×10^{-2}	0.1878	1.575×10^{-2}
	Empirical	0.1254	1.176×10^{-2}	0.1848	1.849×10^{-2}
	Empirical beta	0.1295	1.182×10^{-2}	0.1853	1.027×10^{-2}
	GMMN (NN ₁₀₀ ^{1x})	0.1276	1.162×10^{-2}	0.1819	0.753×10^{-2}
	GMMN (NN ₃₀₀ ^{1x})	0.1089	1.164×10^{-2}	0.1822	1.027×10^{-2}
	GMMN (NN ₆₀₀ ^{1x})	0.1211	1.160×10^{-2}	0.1814	0.753×10^{-2}
	GMMN (NN ₆₀₀ ^{2x})	0.1188	1.166×10^{-2}	0.1809	0.753×10^{-2}
	GMMN (NN ₃₀₀ ^{3x})	0.1219	1.161×10^{-2}	0.1793	0.206×10^{-2}
GBP FX	Independence	0.3591	1.281×10^{-2}	0.3178	6.781×10^{-2}
	Gumbel	0.2241	1.249×10^{-2}	0.2848	1.027×10^{-2}
	Exchangeable normal	0.2197	1.253×10^{-2}	0.2865	0.890×10^{-2}
	Exchangeable t	0.2026	1.224×10^{-2}	0.2713	1.164×10^{-2}
	Unstructured t	0.1371	1.224×10^{-2}	0.2645	0.616×10^{-2}
	Vine	0.1376	1.224×10^{-2}	0.2642	0.343×10^{-2}
	Empirical	0.1245	1.225×10^{-2}	0.2609	0.616×10^{-2}
	Empirical beta	0.1254	1.230×10^{-2}	0.2617	0.890×10^{-2}
	GMMN (NN ₁₀₀ ^{1x})	0.1198	1.209×10^{-2}	0.2560	1.439×10^{-2}
	GMMN (NN ₃₀₀ ^{1x})	0.1154	1.210×10^{-2}	0.2569	0.616×10^{-2}
	GMMN (NN ₆₀₀ ^{1x})	0.1034	1.210×10^{-2}	0.2567	0.068×10^{-2}
	GMMN (NN ₃₀₀ ^{2x})	0.1074	1.209×10^{-2}	0.2544	0.343×10^{-2}
	GMMN (NN ₆₀₀ ^{3x})	0.1247	1.206×10^{-2}	0.2528	1.164×10^{-2}

Table 2 Model assessment metrics for USD (top) and GBP (bottom) exchange-rate data. The AMSE, AVS^{0.25} and VEAR_{0.05} metrics are computed based on $n_{\text{pth}} = 1000$ simulated paths while the AMMD metric is computed based on $n_{\text{rep}} = 100$ realizations.

C Estimation uncertainty in MTS modeling

Establishing theoretical results for our MTS model is challenging. In a time-static setting (i.e., outside the context of MTS), Genest, Ghoudi, et al. (1995) investigated the maximum pseudo-likelihood estimator (MPLE) of parametric copulas. In the context of copula–GARCH models, Chan et al. (2009) studied the MPLE of residual parametric copulas (\hat{C}_{PM} in our framework). In particular, by constructing a weighted approximation to the empirical distribution of (marginal) GARCH residuals, they were able to derive asymptotic normality for the MPLE of \hat{C}_{PM} under regularity conditions, and establish that the derived limiting distribution is independent of the (marginal) GARCH processes. The dimension-reduction step that we used in some applications makes it harder to prove something similar, even for parametric copulas. Moving to \hat{C}_{NN} for our proposed GMMN–GARCH model will require another leap. Even in the static setting, research on statistical inference for generative models is fairly sparse. Farrell et al. (2021) recently derived non-asymptotic high probability bounds on the estimation error of deep neural networks with regression-type loss functions, which, in turn, yielded asymptotic results for subsequent semi-parametric inferences in certain set-ups. However, these results are not easily adaptable to generative neural networks with MMD loss functions.

While some theoretical results in the wider vicinity of the copula–GARCH approach have been established, albeit under conditions not always easy to verify in practice, statistical inference for *generative models* in both static (GMMNs) and dynamic (GMMN–GARCH models) settings remains largely an open problem. For example, the cross-sectional dependence models (Section 2.3) — whether copulas or GMMNs — are trained from $\hat{\mathbf{Y}}_1, \dots, \hat{\mathbf{Y}}_\tau$. The fact that these are estimates themselves introduces additional uncertainty about the resulting models \hat{C}_{PM} , \hat{C}_{NPM} and \hat{C}_{NN} . While Chan et al. (2009) studied the impact on training a parametric copula \hat{C}_{PM} , it seems much harder to develop similar theories for training a GMMN \hat{C}_{NN} .

In this appendix, we conduct an empirical study of this impact by bootstrapping $\hat{\mathbf{Y}}_1, \dots, \hat{\mathbf{Y}}_\tau$. In principle, we could have broadened the scope of our investigation by bootstrapping the original data $\mathbf{X}_1, \dots, \mathbf{X}_\tau$ instead, which would have allowed us to also account for the uncertainties introduced in the first two steps (Sections 2.1 and 2.2). However, cross-sectional dependence has a much subtler effect on the quality of the final probabilistic forecasts than serial dependence does. Therefore, once additional uncertainties about the serial dependence models are considered, it becomes much harder to distinguish various cross-sectional dependence models from one another, which is why we prefer a more focused investigation with a more limited scope.

We draw n_{bt} -many bootstrap samples of size τ , that is, $\hat{\mathbf{Y}}_1^{(b)}, \dots, \hat{\mathbf{Y}}_\tau^{(b)}$, for $b = 1, \dots, n_{\text{bt}}$. The margins are modeled non-parametrically for each of the n_{bt} -many bootstrap samples by computing the pseudo-observations for each sample to obtain $\hat{\mathbf{U}}_1^{(b)}, \dots, \hat{\mathbf{U}}_\tau^{(b)}$, $b = 1, \dots, n_{\text{bt}}$. We then fit n_{bt} -many dependence models (GMMNs or copulas), one for every collection of pseudo-observations. Using these bootstrapped dependence models together allows us to account for the estimation uncertainty associated with modeling $\hat{\mathbf{Y}}_t$. To do so, in Step 2.1) of Algorithm 3.2, we instead generate samples from an equally-weighted mixture of all n_{bt} dependence models. Additionally, the quantile functions associated with each mixture component are utilized in Step 2.2) of Algorithm 3.2.

Using $n_{\text{bt}} = 100$, we conducted the bootstrap experiments on the same data sets from Section 4 for a selected subset of dependence models with varying performance levels — specifically, the single-hidden-layer NN with 300 neurons per layer (NN_{300}^{1x}), the normal copula with exchangeable correlation matrix (N_{ex}), the t copula with unstructured correlation matrix (t_{un}), the vine copula (V), and the empirical copula (\hat{C}). We compared the quality of the empirical predictive distributions produced with and without the bootstrap. Figure 6 displays scatter plots of the AMSE (left column) and AVS^{0.25} metrics for US ZCB yield curves (first row), Canadian ZCB yield curves (second row), USD exchange-rate data

(third row) and GBP exchange-rate data (fourth row). For any given dependence model, the empirical predictive distributions produced with and without the bootstrap showed similar performances. With the bootstrap, the GMMN continued to perform better than the other dependence models.

Our AMSE and $AVS^{0.25}$ metrics are overall assessments of one-day-ahead empirical predictive distributions, averaged across all days $t = \tau + 1, \dots, T$ in the test period. We can also define corresponding daily metrics $MSE(t)$ and $VS(t)$ so that our equations (5) and (6) amount to $AMSE = (T - \tau)^{-1} \sum_{t=\tau+1}^T MSE(t)$ and $AVS^r = (T - \tau)^{-1} \sum_{t=\tau+1}^T VS^r(t)$, respectively, and assess the daily performance ratios with and without the bootstrap, i.e., $MSE_{bt}(t)/MSE_{nbt}(t)$ and $VS_{bt}^{0.25}(t)/VS_{nbt}^{0.25}(t)$, where the subscript “nbt” means “no bootstrap”. Over the entire test period $t = \tau + 1, \dots, T$, both these ratios turn out to fluctuate little around one across all models and datasets considered. Thus, our empirical investigation here suggests that accounting for the uncertainty in the training of cross-sectional dependence models appears to have little impact on the quality of the final probabilistic forecasts produced.

References

- Aas, K. (2016), Pair-copula constructions for financial applications: A review, *Econometrics*, 4(4), 43.
- Aas, K., Czado, C., Frigessi, A., and Bakken, H. (2009), Pair-copula constructions of multiple dependence, *Insurance: Mathematics and Economics*, 44(2), 182–198.
- Alexander, C. (2000), A primer on the orthogonal GARCH model, Manuscript, ISMA Centre, University of Reading, UK.
- Almeida, C., Czado, C., and Manner, H. (2016), Modeling high-dimensional time-varying dependence using dynamic D-vine models, *Applied Stochastic Models in Business and Industry*, 32(5), 621–638.
- Bollerslev, T. (1986), Generalized autoregressive conditional heteroskedasticity, *Journal of Econometrics*, 31(3), 307–327.
- Bollerslev, T. (1990), Modelling the coherence in short-run nominal exchange rates: a multivariate generalized ARCH model, *Review of Economics and Statistics*, 72(3), 498–505.
- Caldeira, J. F., Moura, G. V., and Santos, A. A. P. (2016), Predicting the yield curve using forecast combinations, *Computational Statistics & Data Analysis*, 100, 79–98.
- Chan, N.-H., Chen, J., Chen, X., Fan, Y., and Peng, L. (2009), Statistical inference for multivariate residual copula of GARCH models, *Statistica Sinica*, 53–70.
- Chaudhuri, T. D. and Ghosh, I. (2016), Artificial Neural Network and Time Series Modeling Based Approach to Forecasting the Exchange Rate in a Multivariate Framework, *Journal of Insurance and Financial Management*, 1(5), 92–123.
- Dias, A. and Embrechts, P. (2010), Modeling exchange rate dependence dynamics at different time horizons, *Journal of International Money and Finance*, 29(8), 1687–1705.
- Diebold, F. X. and Li, C. (2006), Forecasting the term structure of government bond yields, *Journal of Econometrics*, 130(2), 337–364.
- Diebold, F. X. and Rudebusch, G. D. (2013), Yield curve modeling and forecasting: the dynamic Nelson-Siegel approach, Princeton University Press.
- Dissmann, J., Brechmann, E. C., Czado, C., and Kurowicka, D. (2013), Selecting and estimating regular vine copulae and application to financial returns, *Computational Statistics & Data Analysis*, 59, 52–69.
- Dziugaite, G.K., Roy, D.M., and Ghahramani, Z. (2015), Training generative neural networks via maximum mean discrepancy optimization, *Uncertainty in Artificial Intelligence-Proceedings of the 31st Conference, UAI 2015*, 258–267.

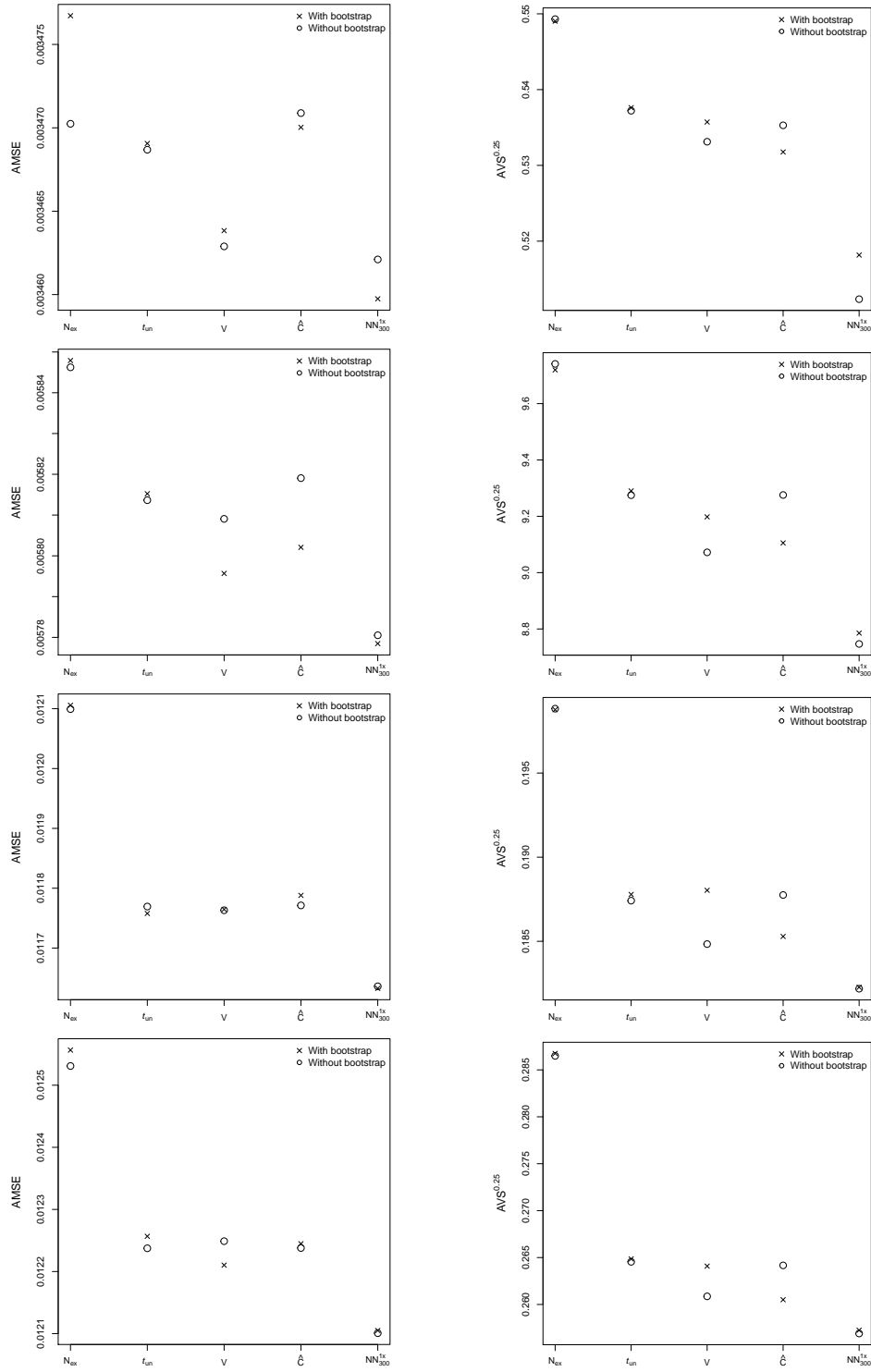


Figure 6 Scatter plots of AMSE (left column) and $AVS^{0.25}$ (right column) for US (first row) and Canadian (second row) ZCB yield curve data, and USD (third row) and GBP (fourth row) exchange-rate data. Each of the eight plots shows a comparison of the empirical predictive distributions produced with (using $n_{bt} = 100$) and without the bootstrap. We see that for every considered dependence model, both methods produce fairly similar quality of empirical predictive distributions according to the two metrics. Moreover, the GMMN models produce the best empirical predictive distributions across all methods and datasets.

- Engle, R. (2002), Dynamic conditional correlation: A simple class of multivariate generalized autoregressive conditional heteroskedasticity models, *Journal of Business & Economic Statistics*, 20(3), 339–350.
- Farrell, M. H., Liang, T., and Misra, S. (2021), Deep neural networks for estimation and inference, *Econometrica*, 89(1), 181–213.
- Genest, C., Ghoudi, K., and Rivest, L.-P. (1995), A semiparametric estimation procedure of dependence parameters in multivariate families of distributions, *Biometrika*, 82(3), 543–552.
- Genest, C. and Segers, J. (2010), On the covariance of the asymptotic empirical copula process, *Journal of Multivariate Analysis*, 101(8), 1837–1845.
- Ghalanos, A. (2019), rugarch: Univariate GARCH models. R package version 1.4-1.
- Glorot, X. and Bengio, Y. (2010), Understanding the difficulty of training deep feedforward neural networks, *Proceedings of the Thirteenth International Conference on Artificial Intelligence and Statistics*, 249–256.
- Gretton, A., Borgwardt, K. M., Rasch, M., Schölkopf, B., and Smola, A. J. (2007), A kernel method for the two-sample-problem, *Advances in Neural Information Processing Systems*, 513–520.
- Gretton, A., Borgwardt, K. M., Rasch, M., Schölkopf, B., and Smola, A. J. (2012), A kernel two-sample test, *Journal of Machine Learning Research*, 13(Mar), 723–773.
- Hinton, G. E. and Salakhutdinov, R. R. (2006), Reducing the dimensionality of data with neural networks, *Science*, 313(5786), 504–507.
- Hofert, M., Kojadinovic, I., Mächler, M., and Yan, J. (2018), *Elements of Copula Modeling with R*, Springer.
- Hofert, M., Prasad, A., and Zhu, M. (2021), Quasi-random sampling for multivariate distributions via generative neural networks, *Journal of Computational and Graphical Statistics*, 30(3), 647–670, doi:10.1080/10618600.2020.1868302.
- Hofert, Marius and Oldford, Wayne (2018), Visualizing Dependence in High-dimensional Data: An Application to S&P 500 Constituent Data, *Econometrics and statistics*, 8, 161–183.
- Jondeau, E. and Rockinger, M. (2006), The copula–GARCH model of conditional dependencies: An international stock market application, *Journal of International Money and Finance*, 25, 827–853.
- Kingma, D. P. and Ba, J. (2014), Adam: A method for stochastic optimization, arxiv.org/abs/1412.6980 (2018-11-01).
- Li, Y., Swersky, K., and Zemel, R. (2015), Generative moment matching networks, *International Conference on Machine Learning*, 1718–1727.
- Ling, C. K., Fang, F., and Kolter, J. Z. (2020), Deep Archimedean Copulas, *Advances in Neural Information Processing Systems*, ed. by H. Larochelle, M. Ranzato, R. Hadsell, M. F. Balcan, and H. Lin, vol. 33, Curran Associates, Inc., 1535–1545.
- Liu, W. K. and So, M. K. P. (2020), A GARCH Model with Artificial Neural Networks, *Information*, 11(10), 489.
- Lua, X., Que, D., and Cao, G. (2016), Volatility forecast based on the hybrid artificial neural network and GARCH-type models, *Procedia Computer Science*, 91, 1044–1049.
- McNeil, A. J., Frey, R., and Embrechts, P. (2015), *Quantitative Risk Management: Concepts, Techniques, Tools*, 2nd ed., Princeton University Press.
- Mercer, J. (1909), Xvi. functions of positive and negative type, and their connection the theory of integral equations, *Philosophical Transactions of the Royal Society of London. Series A*, 209(441-458), 415–446.
- Nelson, C. R. and Siegel, A. F. (1987), Parsimonious modeling of yield curves, *Journal of Business*, 473–489.

References

- Oh, D. H. and Patton, A. J. (2017), Modeling dependence in high dimensions with factor copulas, *Journal of Business & Economic Statistics*, 35(1), 139–154.
- Patton, A. J. (2006), Modelling Asymmetric Exchange Rate Dependence, *International Economic Review*, 47(2), 527–556.
- Patton, A. J. (2012), A review of copula models for economic time series, *Journal of Multivariate Analysis*, 110, 4–18.
- Sancetta, A. and Satchell, S. (2004), The Bernstein copula and its applications to modeling and approximations of multivariate distributions, *Econometric Theory*, 535–562.
- Scheuerer, M. and Hamill, T. M. (2015), Variogram-based proper scoring rules for probabilistic forecasts of multivariate quantities, *Monthly Weather Review*, 143(4), 1321–1334.
- Segers, J., Sibuya, M., and Tsukahara, H. (2017), The empirical beta copula, *Journal of Multivariate Analysis*, 155, 35–51.
- Sklar, A. (1959), Fonctions de répartition à n dimensions et leurs marges, *Publications de L’Institut de Statistique de L’Université de Paris*, 8, 229–231.
- Tse, Y. K. and Tsui, A. K. C. (2002), A multivariate generalized autoregressive conditional heteroscedasticity model with time-varying correlations, *Journal of Business & Economic Statistics*, 20(3), 351–362.
- Yu, J. and Chang, K.-C. (2020), Neural Network Predictive Modeling on Dynamic Portfolio Management—A Simulation-Based Portfolio Optimization Approach, *Journal of Risk and Financial Management*, 13(11), 285.